

This is an Open Access document downloaded from ORCA, Cardiff University's institutional repository:<https://orca.cardiff.ac.uk/id/eprint/131077/>

This is the author's version of a work that was submitted to / accepted for publication.

Citation for final published version:

Blenkinsop, T. G. , Oliver, N. H. S., Dirks, P. G. H. M., Nugus, M., Tripp, G. and Sanislav, I. 2020. Structural geology applied to the evaluation of hydrothermal gold deposits. *Reviews in Economic Geology* 21 , pp. 1-23. 10.5382/rev.21.01

Publishers page:

Please note:

Changes made as a result of publishing processes such as copy-editing, formatting and page numbers may not be reflected in this version. For the definitive version of this publication, please refer to the published source. You are advised to consult the publisher's version if you wish to cite this paper.

This version is being made available in accordance with publisher policies. See <http://orca.cf.ac.uk/policies.html> for usage policies. Copyright and moral rights for publications made available in ORCA are retained by the copyright holders.



Structural geology applied to the evaluation of hydrothermal gold deposits

T. G. BLENKINSOP¹, N.H.S. OLIVER^{2,3}, P. G. H. M. DIRKS², M. NUGUS⁴, G. TRIPP⁵, I. SANISLAV²

1. School of Earth and Ocean Sciences, Cardiff University CF10 3AT UK

2. Economic Geology Research Unit, College of Science and Engineering, James Cook University, Townsville, Queensland 4811, Australia

3. HCOVGlobal, Consultants, PO Box 3533, Hermit Park, Queensland 4812, Australia

4. AngloGold Ashanti, Strategic Technical Group, Perth, Western Australia, 6000

5. PO Box 42, Woodvale, Western Australia, 6026

Corresponding Author: T. G. Blenkinsop, BlenkinsopT@Cardiff.ac.uk

Abstract

The structural geology and tectonic setting of hydrothermal gold deposits are paramount in understanding their genesis, and for their exploration. Strong structural control on mineralization is one of the defining features of these deposits, and arises because the permeabilities of crustal rocks are too low to allow the formation of hydrothermal deposits on realistic time scales unless rocks are deformed. Deformation zones and networks of deformation zones are the fundamental structures that control mineralization. Systematically analyzing deposit geometry, kinematics and dynamics leads to the most thorough comprehension of a deposit. Geometrical analysis relates ore body shape to controlling structures, and networks of deformation zones can be analyzed using topology to understand their connectivity and mineralizing potential. Kinematic analysis determines the location of permeability creation and mineralization. New views of shear zone kinematics allow for variable ratios of pure to simple shear, which change likely directions of mineralization. Multiple orientations of mineralized deformation zones may form simultaneously and symmetrically about the principal strain axes. Dynamic analysis is necessary for a mechanical understanding of deformation, fluid flow and mineralization, and can be achieved through numerical modeling. The relationship between deformation (kinematics) and stress (dynamics) constitutes the rheology: rheological contrasts are critical for the localization of many deposits. Numerous gold deposits, especially the largest, have evidence for multiple mineralizing events that may be separated by tens to hundreds of millions of years. In these cases, reactivation of structures is common, and a range of orientations of pre-existing structures are predicted to be reactivated, given that they are weaker than intact rock. Physical and chemical processes of mineralization can be integrated using a non-equilibrium thermodynamics approach.

Hydrothermal gold deposits form in contractional, strike-slip and extensional tectonic settings. However there may be great variation in the spatial scale over which the tectonic setting applies, and tectonic settings may also change on rapid time scales, so that it is inadvisable to infer local tectonics from deposit-scale patterns, and visa versa. It is essential to place mineralizing events within a complete geological history in order to distinguish pre- and post- mineralizing structures from syn-mineralization deformation features.

Introduction

Structures have been widely recognized as one of the most important controls on hydrothermal gold deposits (Colvine, 1989; Groves and Phillips, 1987; Gustafson, 1989; Robert et al., 1995; Stillwell, 1918; Vearncombe, 1998), and they are commonly regarded as fundamental to exploration (e.g. Weinberg et al., 2004). Nevertheless, some publications on these deposits underemphasize or ignore the role of structures, and lack the detailed mapping that reveals the importance of structure, while in others it becomes a rather exclusive focus. Studies which integrate structural geology with petrography, geochemistry, and geochronology offer the greatest potential insights into ore genesis (e.g. Craw et al., 1999; Kolb et al., 2000; Bateman and Hagemann, 2004; Oliver et al., 2015). A dissenting view of the role of structural geology in gold exploration is offered by Vearncombe and Zelic (2015), who, while advocating the primacy of structural controls, argue that none of 10 structural geology paradigms in the last 60 years have lead to the discovery of gold deposits. These varying perspectives make an interesting context in which to review the role of structures in the formation of hydrothermal gold deposits. Many excellent papers address fluid flow, structures and gold deposits (e.g. Groves and Phillips, 1987; Sibson et al., 1988a; Witt and Vanderhor, 1998; Cox, 1999a), but there does not appear to be a review paper that links geometry, strain, stress and rheology to structural controls on gold mineralization.

Tectonic controls on hydrothermal deposits are also perceived to have profound and commonly simple exploration implications (e.g. Czarnota et al., 2010), such as that gold deposits are associated with particular tectonic regimes or tectonic events. Tectonics is generally considered on a larger scale than structural analysis, which raises important questions about the scales of spatial and temporal variability in tectonic regimes in relationship to tectonic controls on gold mineralization.

The aim of this review is to demonstrate how principles of structural geology can be applied to understanding hydrothermal gold deposits, including some new concepts in structural geology that may be important, although they are not yet widely tested. The question of which spatial and temporal scales are most relevant to the mineralizing processes is discussed through some case studies. An outcome of the earlier parts of the paper is a workflow for applying structural geology to gold deposits. Although some aspects of the review apply to epithermal and Carlin type gold deposits, the emphasis is strongly on lode gold deposits (including associated disseminated deposits; Bierlein and Maher, 2001), which have been commonly described as mesothermal and orogenic (Groves et al., 1998). Intrusion-related gold deposits are not explicitly considered, even

though they may have strong structural controls (Stephens et al., 2004). The deposits described here are bedrock gold deposits (Poulsen et al., 2000), and also “gold-only” deposits (Phillips and Powell, 2015). Problems with classification of gold deposits are considered by Poulsen (1996) and Groves et al. (1998), but are not addressed here.

Why structural geology is so important for gold deposits: Crustal permeability, fluid flow and deformation

Permeability, the material property that links fluid flow to differences in fluid pressure, is central to understanding the structural geology of hydrothermal ore bodies. Permeability in the crust is spatially and temporally heterogeneous and anisotropic (Farrell et al., 2014; Ingebritsen and Manning, 2010). In addition to these inherent problems of characterizing permeability, there are many ways to estimate this property, which give different results: e.g. from the record of geochemical reactions (Dipple and Ferry, 1992), by laboratory measurements (e.g. Brace, 1980), in-situ measurements, and by natural and induced seismic effects. Each of these determinations assesses permeability on different time and spatial scales, in approximately increasing order of scale. Laboratory measurements on cm scale samples are clearly unrepresentative of bulk crustal rock: this discrepancy between lab and in situ measurements is well summarized in Townend and Zoback (2000), who demonstrate that the latter are at least two to three orders of magnitude greater. Determination of the confining pressure effect on permeability has been hampered until recently by experimental procedures (Mitchell and Faulkner, 2008).

Ingebritsen and Manning (2010) therefore distinguish between mean permeability measurements of continental crust, and measurements of elevated, transient crustal permeabilities. The former can be approximated by the Manning and Ingebritsen (1999) empirical calibration of permeability (k , m^2) with depth (z , km), which seems to hold up quite well in comparison to a variety of in situ determinations (Townend and Zoback, 2000):

$$\log k = -3.2 \log z - 14$$

This equation gives typical permeabilities on the order of 10^{-16} to 10^{-18} m^2 for metamorphic rocks in mid to upper crustal conditions (5 – 20 km depth) in which many hydrothermal gold deposits

1 formed. A lower value of 10^{-19} m^2 is calculated from metamorphic reactions (Yardley, 1986).
2 Below 15 km $k = 10^{-18.3} \text{ m}^2$ is a good fit to the data (Ingebritsen and Manning, 2010). With this
3 value, D'Arcy flow of sufficient volume of fluid to form a 10 Moz gold deposit through intact rocks
4 would require 20 to 200 Ma for fluid pressure gradients of 10 to 100 MPa/km (given by the
5 difference between lithostatic and hydrostatic pressures at depths of 5 – 20 km) (see also Cox,
6 1999b).
7
8
9

10
11
12 Transient crustal permeabilities may be estimated (Ingebritsen and Manning, 2010) as:
13
14
15

$$\log k = -3.2 \log z - 11.5$$

16
17
18
19
20
21

22 Below 10 km, transient permeability can be approximated as 10^{-16} m^2 . If these values of transient
23 permeability could be maintained, only 0.9 to 9 Ma would be required to form a 10 Moz gold
24 deposit. A more sophisticated analysis that takes into account time-dependent healing after
25 earthquake-generated permeabilities of 10^{-13} m^2 suggests that such a gold deposit could form within
26 hundreds of thousands of years (Micklethwaite et al., 2015).
27
28
29
30
31
32
33

34 Continuous fluid flow over hundreds or even tens of Ma is probably unrealistic for the formation of
35 even large gold deposits. The above calculations and permeability requirements emphasize why
36 hydrothermal gold deposits require deformation for their formation, and why they are so strongly
37 controlled by structures such as fault and shear zones (e.g. Sibson, 1987; Hodgson, 1989; Poulsen
38 and Robert, 1989; Robert et al., 1995; Cox, 1999b). Permeability may also be created by
39 metamorphic reactions, but these are unlikely to be significant for the formation of ore bodies
40 (Yardley and Cleverley, 2013), although metamorphic fluids have been considered as one of the key
41 transporting agents for gold (Phillips and Groves, 1983; Phillips and Powell, 2015; Pitcairn et al.,
42 2006). “Mobile hydrofractures”, fluid-filled fractures that propagate at ms^{-1} by opening at their
43 upper tip and simultaneously closing at their lower tip (Bons, 2001; Oliver and Bons, 2001), may be
44 another way in which fluids can be transferred rapidly through the crust; these too will have
45 structural controls.
46
47
48
49
50
51
52
53
54
55
56
57

58 Experimental work suggests limitations on the types of deformation-induced permeability required
59 to form gold deposits. Despite pre-failure increases in permeability of two orders of magnitude, in
60
61
62
63
64
65

granites at least permeability is still very low when laboratory samples are loaded up to sample failure (Mitchell and Faulkner, 2008). Even after failure, permeability along fault planes is still not greater than crustal values. These two observations imply that pervasive microcracking may not be adequate to explain permeability requirements for making an ore body, and hence larger scale structures are required. The experiments also indicate the important role of cyclic loading in building up permeability. There is some consistency between these experiments and the damage mechanics models of Sheldon and Micklethwaite (2007). These authors suggest that gold mineralization is hosted on small-displacement structures around jogs in major faults.

While transient, deformation controlled permeability is critical to forming an ore body, comparable issues need to be investigated about alteration patterns, which are typically on a larger scale than the ore bodies, but also reflect fluid-rock interactions.

Applying a Classic Structural Geology Approach to Gold Deposits

A classical approach to structural geology distinguishes 1) geometric description (types, dimensions, orientations, and spacing of structures, and of ore bodies), 2) kinematic inference (displacements, displacement fields and strain) and 3) dynamic analysis (stress), and relates kinematic analysis to dynamics in 4) a rheological analysis (e.g. Tikoff et al., 2013). Successful progression through all four stages would achieve complete mechanical understanding of a problem, but the sequence becomes increasingly difficult to achieve as it is followed through. In the context of ore deposits, kinematic analysis is commonly limited to understanding deformation zone displacements. Dynamic analysis has concentrated on fault-controlled mineralization (e.g. Sibson et al., 1988b), and has otherwise been the preserve of the numerical modeling community (e.g. Mclellan et al., 2007). It is argued below that all three stages are potentially important for understanding ore genesis and for exploration.

Geometry

The geometry of structurally controlled ore bodies can be approximated as planar (related to unconformities, lithological contacts, fractures, veins, deformation zones, fold hinge surfaces) or linear (related to deformation zone bends, stepovers, or intersections, fold hinges, boudin necks) at some scale (Fig. 1). The geometry of planar deformation structures that control gold mineralization can be conveniently divided into those of individual features (fractures/faults, veins, stylolites,

foliations), deformation zones, and groups of deformation zones, or networks (Fig. 2). All of these structures are associated with strain localization at some scale.

Deformation Zones. The description of the deformation zones is a terminological morass. Some of the most problematic issues in describing gold-associated structures are the common use of the words “brittle” and “ductile”, and the definitions and differences between faults, fault zones and shear zones. Imprecision in the use of these words leads not only to confusion but also to fundamental misunderstandings about the relationships of structures to gold mineralization. Figure 3 shows some deformation zones that are associated with gold deposits, and illustrates some of the problems.

“Brittle” and “Ductile” are highly problematic descriptors for several reasons. They have been and still are in use in at least five different ways (Tikoff et al., 2013):

1. In experimental rock mechanics, brittle behavior is contrasted with ductility, defined as a material’s ability to withstand more than 5% permanent strain before failure (Heard, 1960).
2. To distinguish deformation mechanisms e.g. brittle meaning little lattice distortion accompanying fracture (Lawn, 1993) or cataclasis compared to ductile mechanisms such as intracrystalline slip, diffusive mass transfer, or dislocation creep.
3. To distinguish crustal or lithospheric-scale rheology e.g. brittle upper crust, ductile lower crust. The “brittle –ductile” transition separates these rheological domains, and is commonly associated with hydrothermal gold mineralization (e.g. Groves et al., 2003).
4. To distinguish between brittle material that has lost cohesion and ductile material that has not (e.g. Van der Pluijm and Marshak, 2004).
5. To distinguish variations in the displacement field: Brittle deformation meaning discontinuities in the displacement field (e.g. faults) and ductile behavior meaning a progressive change in displacement field (e.g. Twiss and Moores, 2007)).

Definitions 4 and 5 are potentially useful for describing naturally deformed rocks in outcrop. However, “cohesion” is a term that has no ready objective and universal definition, and displacement fields may be hard to define, both factors leading to vagueness in applying these definitions. Another major problem that is hardly ever addressed when brittle and ductile are applied in the field is that they are scale-sensitive (Rutter, 1986). It is common to observe a macroscopically continuous (“ductile”) structure such as a fold that has formed from smaller-scale discontinuities (microfractures, stylolites). Because of the confusion introduced by the different

meanings of the terms brittle and ductile, their lack of precision, and their scale sensitivity, they are not useful for characterizing hydrothermal mineralization. For example, referring to a group of structures on a mine as “the brittle structures” is potentially an important confusion. Which structures would this include, and how are they relevant to the structural controls on an ore body?

Even at a single scale, the type of features shown in Fig. 3C, D pose major terminological problems. These deformation zones have features that are clearly discontinuous at the scale shown, such as faults, and others, such as foliations and folded veins that are continuous at this scale. Such deformation zones are common in mesothermal gold deposits (e.g. Tripp and Vearncombe, 2004; Tunks et al., 2004). They are sometimes referred to as “brittle-ductile shear zones” or “ductile faults”. They commonly have planar, sharp boundaries, outside of which there are zones of alteration up to the width of the deformation zones, which are typically centimeters to meters wide. Within the deformation zones, there is a spectrum from planar to strongly folded veins, which may have en-echelon geometries (Laing, 2004). SC and SC’ fabrics are common, even in zones that have formed at lower greenschist facies conditions (“cataclastic SC fabrics”: Lin, 2001a). Faults are identifiable as slickensided and slickenlined surfaces. There may be porphyroclasts showing typical sigma or delta geometries. Crosscutting relationships and several generations of lineations on single surfaces show that there has been a history of multiple events, involving fabric formation, faulting and veining.

Precision in geometrical description can be achieved by concentrating on continuity and specifying scale. Shear zones can be distinguished from fault zones by continuity at a given scale, and deformation zones that combine continuous and discontinuous deformation at a given scale are logically called “fault-shear zones”. It is important to note that this definition and Fig. 2 are not simply a replacement for the terms brittle and ductile. Continuity, specified at a given scale, is a precise and unambiguous way to describe ore-hosting structures. It is recommended to avoid the use of the terms brittle and ductile: there are several more precise alternatives depending on the context. Some of these alternatives are given above in the analysis of meanings for brittle and ductile: for example, in the context of deformation mechanisms, terminology such as fracture, cataclasis, dislocation creep, diffusion creep or diffusive mass transfer can be used.

Ore Body Geometry. The geometry of ore bodies needs to be understood in order to relate them to the structures and processes that control them. Hydrothermal ore bodies may have very complex

shapes in detail, but many can be simplified into an ellipsoid with maximum (U), intermediate (V) and minimum (W) axes (Blenkinsop, 2004a). By analogy with the strain ellipsoid, it is possible to define the shape of the ore body by the parameter $j = (U/V - 1)/(V/W - 1)$ which divides ore bodies into prolate ($j > 1$) and oblate ($j < 1$) shapes, and to specify the orientation of the ore body through the trend and plunge of the U and W axes. These descriptions can also be used to understand the evolution of the ore bodies, for example by studying how j may change with growth inferred from ore body size (Blenkinsop 2004a); however, since ore body shapes may be influenced by pre-mineralization geometry, and syn- and post-mineralization deformation events, it is important to relate ore body geometry to the whole structural history.

Network Topology. Structural complexity and density of fractures is recognized as important in controlling gold mineralization potential (e.g. Tripp and Vearncombe, 2004). More specifically, the geometry of networks of deformation zones controls ore bodies on scales larger than the individual deformation zones. Network geometry is usually described by attributing the component orientations into sets, and measuring the spacing, frequency, density or intensity of traces of deformation zones (Dirks et al., 2013; Riley, 2005). However, traces can be ambiguous to interpret where there is splaying. For example, at the intersection of the three branches indicated by “?” on Fig. 4, a vein trace splits and it is unclear which branch belong to the same unique trace. Traces are subject to a greater amount of sampling bias (censoring) (Sanderson and Nixon, 2015), and trace analysis does not capture the topology of networks, which is critical for measuring connectivity. Topological analysis of networks focuses on branches, defined as segments of a trace between nodes, where the trace either terminates, or joins two or three other branches (Fig. 4). These locations are I, Y and X nodes respectively, and the proportions of each type of node characterize the network topology. The average number of connections per branch (C_B) partly characterizes network connectivity (Sanderson and Nixon, 2015). Since each Y node connects to 3 branches, and each X node to 4,

$$C_B = (3N_Y + 4N_X)/N_B$$

Where N_Y , N_X , and N_B are the number of X and Y nodes and branches respectively. Thus in Fig. 4. $C_B = (30 + 12)/28 = 1.5$. This number seems to be typical of a number of natural fracture networks. Topological measures such as C_B are independent of any scale.

However, the permeability of a network will depend not only on relative numbers of different types of nodes, but also the intensity of the branches, as assessed by their number or length per unit area or area per unit volume. Both connectivity and intensity can be measured from branch analysis, and can be combined to characterize the likely permeability properties of the network (Sanderson and Nixon, 2015). This type of analysis, developed in three dimensions, would seem highly suited to evaluating the resource potential of stockworks. Network analysis is closely aligned to percolation theory (Stauffer and Aharony, 1994), which has interesting potential for understanding hydrothermal mineralization (Blenkinsop, 2014). Networks are also useful to describe 3D model topologies (Thiele et al., 2016a, 2016b).

Network topology may also be one way to probe an enigma posed by the relationship between hydrothermal gold deposits and first and lower “order” structures. A common view is that gold deposits are hosted in lower (second, third etc.) order structures adjacent to, but not on, first order (major) structures (Eisenlohr et al., 1989; Blenkinsop et al., 2000; Weinberg et al., 2004). Lower order structures correspond to dangling elements in a network (Cox, 1999). In the above terminology, these are branches that join I to Y or X nodes. The location of gold deposits on lower order structures is attributed to the greater opportunities for fluid-rock interaction or fluid mixing afforded by these structures. However, there are several examples where the largest regional structures do host important gold deposits, including the Ashanti deposit at Obuasi (Blenkinsop et al., 1994; Allibone et al., 2002a) and deposits at Bogoso (Allibone et al., 2002b), both in Ghana, and Kerr Addison, Kirkland Lake, Canada (Jia and Kerrich, 2000). Considering the deformation zones as networks and analyzing the branch geometry would be an effective way to test the relationship of deposits to structural hierarchy, and to determine if there is indeed a general pattern. An important consideration for implementing network analysis is to demonstrate that the analyzed deformation zones were simultaneously active, and that the pattern is not a product of overprinting or selective reactivation of older structures or lithostratigraphic contacts.

Kinematics

The kinematics of deformation zones and networks during mineralization, in combination with their geometry, determine sites of deformation-enhanced permeability. Dilational stepovers (jogs) and bends in deformation zones (e.g. Weinberg et al., 2004) are commonly regarded as particularly favorable for mineralization, but fracturing and permeability are also created at contractional stepovers and bends (e.g. Ford et al., 2009). Deformation zone roughness or non-planarity can

therefore be an important aspect of prospectivity. Deformation zones represent crustal weaknesses that may be reactivated many times. Distinguishing between pre-, syn- and post-mineralization kinematics is therefore important, especially when mineralization has occurred in repeated events or gold has been remobilized. Mineralization needs to be placed in a complete kinematic history by analysis of relative age via overprinting relationships and timing compared to geological events such as intrusions (e.g. Miller and Wilson, 2004), and by absolute age dating (e.g. Morelli et al., 2010). A rigorous application of structural geology to understanding hydrothermal mineral deposits results in terminology (D_1 , D_2 , D_n , S_1 , S_2 , S_n , L_1 , L_2 , L_n etc. e.g. Table 1) that can appear to verge on jargon to the non-specialist, but in many cases this notation is an efficient if not essential way to present a complex spatio-temporal sequence in an orderly fashion. New understanding of the kinematics of individual deformation zones, and their networks, has special significance for interpreting syn-kinematic mineralization as described below.

General Shear. A new perception about the kinematics of individual shear zones has developed over the last 25 years, which focuses attention on relationships between the foliation, shear plane, shear direction, direction of maximum elongation (lineation), and the vorticity vector. The vorticity vector in particular is a key concept, which can be thought of informally as the “rolling axis” in shear (Fig. 5). Previously the paradigm for shear zones was based on the Ramsay and Graham (1970) model that shear zones were localized zones of inhomogeneous simple shear, in which the lineation and shear direction are perpendicular to the vorticity vector. However, observations and models of shear zones where the lineation is parallel to the vorticity vector contradict the perpendicular relationship predicted by the Ramsay and Graham model, and these situations have instead been explained by models with significant components of pure shear (Fig. 5, e.g. Tikoff and Fossen, 1993; Fossen, 1993; Tikoff and Greene, 1997; Tikoff and Fossen, 1999). Many of these models were framed in the context of transpression (Sanderson and Marchini, 1984; Jones and Holdsworth, 1998; Lin et al., 1998). Possibilities of even more variable relationships among foliation, lineation, shear direction and the vorticity vector have resulted from further work, including those of triclinic shear (Jiang and Williams, 1998; Lin et al., 1998). These advances have yet to be fully incorporated into studies of mineralized shear zones (but see Lin, 2001b), so that it is unclear how widely general shear has affected gold deposits, but the following examples demonstrate that where a new appreciation of shear zone kinematics has been applied, it has had profound consequences for understanding syn-mineralization deformation.

The importance of pure shear components is illustrated by the Taurus shear zone at Golden Pig

mine, Southern Cross Greenstone belt, Yilgarn craton (Nugus et al., 2003). The Taurus Lode at Golden Pig is hosted by an intensely deformed sequence of predominantly mafic and ultramafic rocks with intercalated Banded Iron Formations (BIF) and sedimentary rocks. The Taurus shear zone comprises a zone of steeply WSW dipping schistosity (S) with a strong biotite, amphibole and pyrrhotite lineation (L) plunging 10° S. Underground exposures show the kinematics of the shear zone very clearly. On drive headings, perpendicular to the foliation and lineation, there is consistent evidence for reverse shear, while roof views parallel to the lineation and perpendicular to the foliation show sinistral and dextral asymmetries, from deformed veins. The vorticity vector appears to be parallel to the lineation, suggesting a pure-shear dominated shear zone, with a reverse component (Fig. 6). The large amount of flattening may be related to the position of the shear zone between two adjacent granite domes. Ore body long axes (*U* axes) plunge parallel to the lineation and vorticity vector (Nugus et al., 2003).

Another example where pure shear may be dominant is part of the Arcturus deposit in the Shamva greenstone belt, Zimbabwe. The pyrrhotite-arsenopyrite-pyrite ore bodies are hosted in a network of shear zones up to 1 km wide, defined by S – L fabrics of biotite-actinolite-quartz-epidote-fuchsite (Mutemeri, 2001). Shear zones dip steeply to the N or NE, and ore body *U* axes and lineations also plunge in this direction in the Ceylon section of this mine (Fig. 7). However, dextral asymmetries are seen in plan view, suggesting a vorticity vector plunging parallel to the lineation, and a dominant component of pure shear (Blenkinsop, 2004a).

These situations contrast with mineralized shear zones dominated by simple shear, as illustrated by two more examples from Zimbabwe. In the Renco mine, Northern Marginal Zone of the Limpopo belt, the major ore bodies are hosted within four main shear zones 0.1 to 3 m wide dipping gently to the southeast (Blenkinsop and Frei, 1996). Shear zones consist of quartz-feldspar-biotite-hornblende mylonites and garnet-biotite-feldspar-quartz tabular pods where pyrrhotite, chalcopyrite and pyrite are associated with mainly free gold (Kisters et al., 2000; Kolb et al., 2000). Mineral stretching lineations plunge down dip (Fig. 7). Clear shear sense indicators are seen on planes parallel to the lineation and perpendicular to the foliation, giving a reverse sense of shear in the north part of the mine (Kisters et al., 1998). The *U* axes of ore bodies plunge generally to the southeast (Blenkinsop and Kadzviti, 2006), parallel to the lineations and perpendicular to the inferred vorticity vector (Fig. 7). These kinematics are compatible with the observed thrust sense of movement of the Northern Marginal Zone over the Zimbabwe craton, which occurred at the end of the Neoproterozoic (Blenkinsop et al., 2004), and with simple-shear dominated kinematics. The oblate

1 shapes of these ore bodies, and their orientation parallel to the lineation, can be explained by higher
2 permeabilities within the shear zone and parallel to the shear direction. Variations in the ore body
3 orientation may reflect a process of ore body growth by coalescence (Blenkinsop and Kadzvi, 2006).
4
5
6
7

8 The Shamva mine in the Harare-Shamva greenstone belt, Zimbabwe, is another example of a
9 deformation zone hosted gold deposit with simple-shear dominated kinematics, but with a different
10 arrangement of ore bodies and shear directions compared to the Renco case. The Shamva ore
11 bodies are hosted in the sub-vertical NE-trending Shamva shear zone, which has a sinistral strike-
12 slip sense of shear (Jelsma et al., 1998). The shear zone consists of a network of principal (Y) and
13 Riedel (R) shears, which intersect in steeply plunging lines, and show a typical strike-slip
14 configuration. The *U* axes of the pyrite-carbonate ore bodies with an alteration assemblage of
15 biotite-tourmaline-oxide-carbonate-quartz plunge steeply, perpendicular to sub-horizontal
16 slickenfibres lineations (Blenkinsop, 2004a). The ore bodies formed along shears in R and Y shear
17 orientations, and at their intersections. In this case the ore bodies are parallel to the vorticity vector
18 and perpendicular to the lineation, in contrast to the situation at Renco, where ore bodies are parallel
19 to the lineation but perpendicular to the vorticity vector.
20
21
22
23
24
25
26
27
28
29
30

31 The three studies illustrate three different types of kinematic control through three possible relations
32 among ore bodies, lineations and vorticity vectors (Figs. 5, 7). In the pure shear dominated cases of
33 Golden Pig and the Ceylon section of the Arcturus deposit, ore body *U* axes form parallel to the
34 lineation and the vorticity vector. In the simple shear dominated cases of Renco and Shamva, there
35 seem to be two possibilities. At Renco, ore body *U* axes are parallel to the lineations and
36 perpendicular to the vorticity vector (Fig. 7). They formed in such an orientation because of
37 enhanced permeability in the shear zone fabric. In contrast, at Shamva, the *U* axes are perpendicular
38 to the lineations and parallel to the vorticity vector. The control on the ore bodies may also have
39 been permeability, but in this case the greatest permeability was along intersections between shears,
40 which are parallel to the vorticity vector and perpendicular to the lineations (Fig. 5C, 7C).
41
42
43
44
45
46
47
48
49
50
51

52 The relationships between ore bodies, lineations and vorticity vectors may partly be a function of
53 metamorphic grade: there is a need for more systematic documentation of these relationships to
54 explore this further. It is also important to note that progressive deformation can lead to
55 overprinting relationships within the same deformation event (e.g. as material lines rotate from
56
57
58
59
60
61
62
63
64
65

shortening to lengthening fields), and that post-mineralization deformation may affect ore body geometry and therefore interpretations of kinematic controls on ore bodies. Additional complications in kinematic interpretations can also be expected where there have been multiple mineralizing events in the same deposit (see below).

Conjugate and Polymodal Networks. Deformation zones may form conjugate or polymodal geometries that are symmetrical about bulk principal strain axes, and hence control mineralization in systematic patterns. Conjugate faults, that is two orientations symmetrically disposed at acute angles to the maximum shortening direction, dominate conceptions of how faults interact (cf. Anderson, 1905). However, such conjugate faults can only accommodate plane strain (Healy et al., 2015). Experiments (e.g. Oertel, 1965; Aydin and Reches, 1982), field observations (Woodcock and Underhill, 1987; Oesterlen and Blenkinsop, 1994; Carvell et al., 2014), and theory (Oertel, 1965; Reches, 1983), by contrast, emphasize that fault networks are polymodal, consisting of four orientations (quadrимodal) of simultaneously active faults, or a dispersion of orientations (Fig. 8). Intersections between polymodal networks of faults can have complex geometries (Healy et al., 2015). Quadrимodal patterns have also been reported for deformation bands (Underhill and Woodcock, 1987) and kink bands (Kirschner and Teixell, 1996). The formation of quadrимodal kink bands was contemporary with mineralization at Bendigo, Victoria, and these kink bands control mineralization on millimeter to kilometer scales (Raine, 2005).

Shear zone networks may form in conjugate pairs (Mitra, 1979) but they also commonly have orientations that are more varied, forming networks that isolate lozenges of less-deformed rock, which approximate the shape of the strain ellipsoid (Fig. 8: Choukroune and Gapais, 1983; Gapais et al., 1987; Kruckenberg et al., 2010). These patterns can accommodate general shear (Hudleston, 1999). Quadrимodal shear zone networks were demonstrated to control ore bodies at the very high gold grade Norbeau deposit, Quebec (Dube et al., 1989). Here, quartz veins occur in four sets of shear zones within a metamorphosed layered mafic intrusion. The shear zones are compatible with a single strain field, which consists of down-dip extension of the sill and strike-parallel shortening. The orientation of the sill appears to have guided the principal strains because of its competence.

Polymodal patterns of deformation zones have major implications for understanding of the basic principles of deformation and for ore body geometry. Since polymodal faults and shear zones have clear relationships to strain ellipsoids and non-plane strain, it is evident that kinematics are

fundamental to both faulting and shearing, including deformation bands and kink bands (cf. Marrett and Allmendinger, 1990; Hudleston, 1999; Healy et al., 2015). The patterns of deformation zones shown in Fig. 8 are similar in: i) having an orthorhombic symmetry about the bulk principal strain axes and ii) having four clusters (or orientations distributed around four modes). These similarities argue for a kinematic “control” on deformation zones. The bulk strain patterns accommodate non-plane strain (Healy et al., 2015), and, at least for faults, form in true triaxial stress conditions (Chang and Haimson, 2012), which are likely to be common in the crust (Lisle et al., 2006).

Polymodal patterns of deformation zone networks may be more widespread than generally appreciated, for the reasons suggested in Healy et al. (2015). Because the recognition of the generality of polymodal patterns is recent, their implications for ore bodies are not widely known, but at least in some cases it is evident that ore bodies may form along the four orientations of the deformation zones (Raine, 2005; Dube et al., 1989). One may also predict that shoots may be localized along the four directions of intersections of polymodal deformation zones because they are directions of enhanced permeability.

Dynamics

It is difficult to overemphasize the importance of the fault valve model (Sibson et al., 1988) for the insights that it has brought to the dynamic understanding of gold mineralization. Four major perceptions that come from this model are:

- 1) Transient permeability for large fluid fluxes is created by movement on deformation zones. This has obvious exploration implications: geometries of favorable deformation zones may combine continuous and discontinuous deformation, as commonly observed (e.g. Robert et al., 1995).
- 2) Reactivation and repeated deformation characterize the formation of ore bodies. This point has important implications for deciphering structural histories, in which changes in kinematics and stresses during a mineralizing event should not be mistaken for longer-term distinct orogenic episodes.
- 3) Fluid pressure fluctuations, perhaps associated with the seismic cycle and involving supralithostatic pressures, are critical. This point suggests that unfavorably orientated structures, requiring high fluid pressures for reactivation, may be preferred structures for ore bodies.

- 4) Fluid pressure decrease leads to gold precipitation. This mechanism may explain contrasting styles of ore bodies in the same deposit. Vein hosted gold may form by pressure decrease, while replacement ore may form from fluid-rock interaction.

The link established by the fault valve model between gold mineralization and the seismic cycle leads naturally to the application of Coulomb stress, or stress transfer, modeling (Cox and Ruming, 2004). This type of modeling simulates the static stress changes that would be associated with seismic movement of a given fault geometry. Application to the St Ives gold field, Yilgarn craton shows how the location of gold mineralization corresponds to the predicted position of aftershocks from a main shock rupture on the adjacent Bolder-Lefroy fault system (Micklethwaite and Cox, 2004; 2006). The aftershocks created zones of high permeability. An attractive aspect of this hypothesis is that it explains the common observation that mineralized structures for lode gold style deposits in particular have low displacements, and occur adjacent to major structures. It is important to establish that all faults included in the model were active at the time of mineralization.

Finite element modeling (FEM) has also proven of value in understanding hydrothermal gold deposits (Holyland and Ojala, 1997; Schaub et al., 2006; Schaub and Zhao, 2002). McLellan et al. (2007) show how structural analysis can be used to infer stress conditions leading to failure on shear zones. Applying these stress conditions leads to predictions of volumes of high shear strain, dilation and most likely failure, which have important exploration applications. An important part of the modeling is to include the effect of the stress ratio, $\Phi = (\sigma_2 - \sigma_3)/(\sigma_1 - \sigma_3)$ (Angelier, 1975), which varies from 0 for $\sigma_2 = \sigma_3$, to 1 for $\sigma_1 = \sigma_2$. Table 1 shows how variable Φ values were used during the tectonic history at Sunrise Dam; taking this into account made a significant difference to the modeling results. Another illustration of the importance of dynamic analysis comes from the Magdala gold deposit, in the Lachlan fold belt, Victoria (Miller and Wilson, 2004a). By reconstructing the stress history from fault slip measurements, the existence of a displaced footwall ore body (the Golden Gift ore body) was predicted, based on the position of the hanging wall Magdala ore body that was being mined. It was possible to establish a detailed stress history; again, the stress ratio Φ had significant effects, in this case on predicted fault slip directions. However, application of FEM models becomes considerably more complex, and less predictive, when the effects of varying strain rates, heating, chemical reaction and permeability are considered, and when 2D modeling is applied to 3D situations.

1 It is puzzling that Coulomb stress modeling and FEM both appear to be successful, since the first
2 considers only stress changes caused by increments of slip, and the second uses a constant remote
3 applied stress and does not take into account changes in stress due to discrete slip events. This
4 paradox leads to an important uncertainty about mechanical models for hydrothermal gold deposits.
5 Faults have been regarded as either slipping seismically (Coulomb stress modeling) or creeping
6 aseismically (FEM), but recently it has become clear that there is a spectrum of fault slip modes that
7 include seismic slip, episodic tremor and slip, slow earthquakes, and fault creep (e.g. Ben-zion,
8 2008; Gomberg, 2010; Beroza and Ide, 2011). Although many of the relevant observations come
9 from the Cascadia and Nankai subduction zones, similar phenomena are now recognized on normal
10 faults in rifts (Calais et al., 2008), and in the San Andreas fault and other strike-slip and oblique slip
11 fault systems (Chamberlain et al., 2014; Jolivet et al., 2014). Continuous, aseismic sliding (creep)
12 has now been observed, thanks to more extensive geodetic coverage, on a variety of types of faults
13 around the world, at speeds up to those of plate motions (10^{-9} ms⁻¹). Observations of fault slip
14 between the extremes of seismic and continuous aseismic modes have collectively been termed
15 slow-slip phenomena, and are recognized as components of a continuum of fault behavior (Peng
16 and Gomberg, 2010). The fundamental controls on the spectrum of fault slip modes and speeds are
17 not known.

18
19
20
21
22
23
24
25
26
27
28
29
30
31
32 The phenomenology of slow slip makes it likely to be important in gold mineralization. Seismic
33 signals associated with slow-slip events indicate that they are due to slip on faults, like earthquakes.
34 It is very likely that pore fluids at high pressures are involved (e.g. Chamberlain et al., 2014).
35 Moreover, there is field evidence to support the link between slow slip and gold mineralization.
36 Fagereng and Sibson (2010) demonstrated that mixed continuous-discontinuous deformation zones
37 observed in the field, comparable to fault-shear zones that host gold (e.g. Fig. 3C, D), may have the
38 correct physical properties for different types of fault slip. Furthermore, veins with similar crack-
39 seal textures to those seen in gold deposits (e.g. Boullier and Robert, 1992; Robert et al., 1995),
40 have the correct geometrical properties to generate the episodic tremor that is associated with slow
41 slip events (Fagereng et al., 2011). The possibility of slow slip as a hydrothermal gold
42 mineralization mechanism has not been widely considered, or included in numerical models for
43 mineralization.

44 45 46 47 48 49 50 51 52 53 54 55 56 57 58 59 60 61 62 63 64 65 **Rheology**

The determination of relationships between deformation and stress, “rheology” in the broadest

sense, is perhaps the most difficult part of a structural analysis, since about the only aspect of a complex ore deposit that can be well constrained is generally the present geometry, allowing estimates of some displacements and strain. Common methods of dynamic analysis for the reduced stress tensor are limited to discontinuous deformation; strain rates are commonly unknown, and material properties at the time of deformation can be little more than guesses. Despite these limitations, rheological explanations for mineralization are some of the most commonly invoked, perhaps because of the obvious localization of mineralization along rheological contacts or within units with distinct rheology. A good example comes from Renco gold mine, Zimbabwe, for which the kinematics were described above. Gold mineralization within mylonitic shear zones developed at mid-upper amphibolite facies is concentrated in meter-wide competent lithons consisting of an alteration assemblage of quartz, feldspar biotite and garnet which has veins, fractures, breccias and abundant sulphides, mainly pyrrhotite (Kisters et al., 2000; Kolb et al., 2000). These lithons are mineralized because they fractured, creating dilatancy, compared to the flow in the adjacent protomylonites and mylonites. Fracturing may have occurred during seismic events. A much larger scale rheological control is seen in the localization of mineralization the around the Scotia-Kanowna Dome, in the east Yilgarn craton, Australia. There, the world-class Kanowna Belle deposit was formed because mineralizing fluids were focused into a dilatant volume at the nose of the Scotia-Kanowna Dome (Davis et al., 2010a). Smaller deposits were also formed in shear zones localized around the sides of the dome. The same rheological contrasts may account for patterns of mineralization in other parts of the Yilgarn craton. Sites of low mean stress have the potential to focus fluid flow and may have negative fluid pressures, resulting in extensional veining and dilation (Ridley, 1993).

Reactivation and Multiple Mineralizing Events

It is obvious from many hydrothermal gold deposits that structures that formed in earlier tectonic events are reused by fluids and localize mineralization during a subsequent deformation/mineralization event. A clear signpost to the importance of such reactivation is syn-mineralization deformation of zones in “unfavorable” orientations i.e. orientations that have lower ratios of shear to normal stress than the optimum orientation (Fig. 9). A classic example are the high angle reverse faults in the Sigma mine, Canada, which originated as normal or strike slip faults (Sibson et al., 1988), and required supralithostatic pore fluid pressures for reactivation (Boullier and Robert, 1992). Another example is provided by the St Ives goldfield, Western Australia, where a set of WNW trending faults links mineralized N-trending faults (Miller et al., 2010). The WNW trending faults correspond to isopach thickness variations and so were probably active as normal faults

during basin formation, 50 Ma earlier than gold mineralization. A third example comes from the Kainantu gold mine in Papua New Guinea (Blenkinsop et al., 2017). Gold-copper mineralization with classic epithermal textures occurs in NW-SE steeply dipping veins. These veins are developed along a dextral strike slip shear zone network, which itself is generally parallel an earlier greenschist facies cleavage in the host rocks. High Au grades correlate with areas of obliquity between the shear zone fabrics and the cleavage, and plunge at $\sim 40^\circ$ southeast parallel to hinges of a crenulation cleavage. The cleavage could be as old as the Jurassic; mylonitization and crenulation may date between 40 Ma and 9 Ma, and mineralization is probably related to an extensional phase of deformation at 9 – 6 Ma. Mineralization was followed by strike-slip faulting in the same orientation as the mineralized veins that is compatible with the current N-S convergence, which has been ongoing for the last 4 – 5 Ma. The relatively recent and well-preserved geological history at Kainantu allows a detailed history of reactivation to be deciphered and related to the tectonic history. In this case reactivation of fabrics, shear zones and veins with the same orientation has occurred over as long as 200 Ma in at least 4 discrete events.

A general prerequisite for reactivating faults is a reduction in either or both cohesion and coefficient of internal friction along the reactivated fault (Fig. 9), otherwise new faults will form in intact rock rather than older structures being reactivated. In all cases it is apparent that a range of orientations can be reactivated for a fault that is weaker than intact rock, in a given stress state. Reactivation may therefore be common where there are pre-existing discontinuities in a variety of orientations. For very unfavorable orientations, reactivation will require supralithostatic pressure (Sibson, 1985).

The reactivation potential of cohesionless faults is conveniently analyzed by the slip and dilation tendencies. Slip tendency measures the propensity for a fault to reactivate in shear, and dilation tendency is the propensity for extensional reactivation (Moeck et al., 2009; Morris et al., 1996). The tendencies can be normalized to frictional properties so that the most favorable orientation for reactivation has a tendency of 1 and the least favorable (no reactivation) has a tendency of 0 (Lisle et al., 2006; Moeck et al., 2009). An advantage of this method for analyzing reactivation is that it shows clearly how the relative value of the intermediate stress has a major effect on the pattern of expected reactivation (Morris and Ferrill, 2009) (Fig. 10). Given that the most common state of stress in the crust has $\Phi = 0.3$ (Lisle et al., 2006), any fault at angles of $20\text{--}40^\circ$ to σ_1 has a high slip tendency, while a range of orientations of faults sub-parallel to σ_1 have high dilation tendencies (Fig. 10).

While it may seem intuitive that a pre-existing fault has lower strength, experiments indicate that crack healing and strength recovery can be rapid (on the order of hours at high temperatures) due to compaction and cementation (Smith and Evans, 1984). However, reduction in permeability also has the effect of increasing pore fluid pressures, facilitating failure (Tenthorey et al., 2003). There is therefore likely to be feedback between deformation, permeability creation, pore fluid pressure, fluid movement and cementation, possibly creating complex behavior on reactivated faults (Barnhoorn et al., 2010).

Advances in dating mineralization have made it clear that the endowment of several major gold deposits or goldfields has accumulated in distinct events separated by tens or even hundreds of millions of years. For example, Frei et al., (1998) showed that Archean gold mineralization at 2.60 Ga in the Kimberly-RAN mines in Zimbabwe was followed by Early Proterozoic gold deposition at 1.96 Ga. In the central Victorian goldfield, Australia, initial gold mineralization occurred in the Late Ordovician, during the early stages of the accretionary development of the Lachlan fold belt, followed by Late Devonian mineralization at 376 Ma (Arne et al., 2001). In the Meguma terrane, Nova Scotia, mineralization occurred at two times in the Devonian, 407 Ma and ca. 380 Ma (Morelli et al., 2005). These are correlated with regional Acadian orogenesis and granite intrusion/high grade metamorphism respectively. Reactivation is likely to be a key to adding extra resources in situations of multiple mineralizing events.

Thermodynamics: An integrated approach

A systems approach to hydrothermal gold mineralization has been advocated for some time (Fyfe and Kerrich, 1976; McCuaig and Hronsky, 2016; Wyborn et al., 1994) but many studies are qualitative and have focused on exploration implications rather than genetic understanding of mineralization (Wyman et al., 2016). The systems approach clarifies that the formation of an ore body involves many feedbacks and is likely to be highly non-linear (Ord et al., 2012). Non-equilibrium thermodynamic approaches to deformation (Hobbs et al., 2012) and mineralization (Ord et al., 2016, 2010) offer a chance to quantify a systems analysis and to use it to understand the fundamentals of forming an ore body (Fig. 11). The model proposed by Ord et al. (2012), Lester et al. (2011) and Hobbs and Ord (2017) treats ore body formation as an open system reactor in which a sustained flux of reactants and energy creates alteration through exothermic reactions initially, which subsequently undergo competition from endothermic ore precipitation reactions. Deformation, fluid transport, heat and chemical reactions are all coupled (Fig. 11). A prediction of

this approach is that ore bodies are multifractal and have spatial scale invariance (Munro et al. 2017).

Spatial and temporal variability in tectonic controls on hydrothermal gold deposits

Compressional and transpressional tectonic controls on gold mineralization at local and regional scales are widely documented (e.g. Groves et al., 1998; Goldfarb et al., 2001; Goldfarb et al., 2005). However, there are many examples that show how extensional and strike slip tectonic settings at a variety of scales may also be important, illustrated in the following case studies. The Shamva shear system described above has a Riedel geometry that is consistent with sinistral simple shear, and no shortening component to render it transpressional (Jelsma et al., 1998; Blenkinsop, 2004a). Sunrise Dam is one of Australia's premier gold mines, situated in the Laverton greenstone belt on the Yilgarn craton, and hosted in andesitic to basaltic volcanoclastic rocks, iron formation, turbidites and porphyry sills and dykes. In several respects Sunrise Dam Gold Mine is a typical greenstone-hosted, late Archean lode gold deposit. As usual for a world-class resource, there are several styles of mineralization and important variations through the mine among shear zone-, stockwork-, breccia- and vein-hosted mineralization. The rocks experienced a complex structural sequence with mineralization occurring under greenschist facies conditions in the Late Archean (Baker et al., 2010). The deformation/mineralization sequence involves at least two major episodes of mineralization during D₄ (Table 1), which was characterized by dextral-normal extensional shear (Blenkinsop et al., 2009), accompanied by a late CO₂ fluid influx associated with Te, Ag, and As (Sung et al., 2007; Baker et al., 2010). A more recent example of strike-slip dominated lode gold mineralization is provided by the latest Eocene-Oligocene mineralization in the Daping gold deposit, containing one of the largest resources in the Ailaoshan gold belt, Eastern China, which is related to the right lateral Red River fault (Hou and Cook, 2009; Sun et al., 2009).

Clear examples of hydrothermal gold mineralization during extension, well below the top 2 km of the crust where epithermal deposits form, are reported from the Dolgelau Gold Belt in North Wales, where the Clogau-St Davids (100 000 oz Au produced) and Gwynfynydd (50 000 oz Au) mines are located (Platten and Dominy, 2009). The gold-bearing quartz veins in the gold belt consist of an ENE-WSW array of steeply dipping laminated quartz-carbonate veins hosted in Cambrian mudstones at low greenschist facies conditions (Dominy et al., 1996a, b). The veins are hosted within normal faults that pre-date the veining. Originally considered to have a late to post-tectonic

1 timing (Shepherd and Allen, 1985), detailed work by Platten and Dominy (1999) shows that the
2 gold mineralization predates an Acadian slaty cleavage. A critical piece of evidence is the presence
3 of barren lenticular quartz veins, which cross-cut the gold-bearing quartz veins, and are related to
4 the sub-horizontal shortening and sub-vertical extension of the cleavage and fold forming event.
5 The barren quartz veins also cut post-mineralization “Clogau Stone” dykes, confirming the early
6 timing for the mineralization. Narrow zones of alteration around the veins include phyllosilicates,
7 carbonate and silica (Dominy et al., 1996a, b). Low salinity aqueous-CH₄- CO₂ fluids suggest ore
8 formation at 300-320°C, 180 MPa (Bottrell et al., 1988). Gold precipitation was by destabilization
9 of either chloride or sulfide complexes, as a result of fluid interaction with host-rock graphite
10 (Shepherd et al., 1991). The veins formed due to fluid overpressure in an NNW-SSE extensional
11 event, contemporary with Ordovician volcanism and development of the Lower Paleozoic Welsh
12 basin (Kokelaar, 1988) that predates the Acadian orogeny.
13
14
15
16
17
18
19
20
21
22

23 Detailed structural analysis of several hundred mine working in the Barberton greenstone belt
24 shows that almost all mineralization was associated with normal faulting, with a dominantly NW-
25 SE extension direction. This mineralization event is dated at ~ 3015 Ma, 85 Ma after granite
26 batholith emplacement and stabilization of the craton, at the time that the Witwatersrand basin
27 opened (Dirks et al., 2013, 2009; Munyai et al., 2011). In large mines like Sheba and New Consort
28 (together > 6Moz) in Barberton, the normal faults overprint/reactivate thrusts that were linked to
29 accretionary events which occurred ~200 Ma before gold mineralization. In the Nyankanga gold
30 deposit (~10 Moz), Geita greenstone belt, Tanzania, mineralization occurred during normal
31 reactivation of the reverse Nyankanga fault-shear zone (Sanislav et al., 2015), and at the Geita Hill
32 gold deposit (~3 Moz), there is evidence to link at least some of the mineralization to normal fault
33 movement in the last deformation event recorded in the deposit which appears to have occurred
34 ~40-50 Ma after the accretionary stages in the greenstone belt (Sanislav et al., 2017). This is well-
35 illustrated by sub-vertical, approximately E-W trending, mineralized quartz veins that overprint
36 earlier structures and are surrounded by a gold-rich alteration halo of quartz, biotite, k-feldspar and
37 pyrite (van Ryt et al., 2017).
38
39
40
41
42
43
44
45
46
47
48
49
50
51
52

53 Extensional structural controls on gold mineralization in the Yilgarn craton have been advocated by
54 several studies (Davis and Maidens, 2003; Czarnota et al., 2007; Weinberg and van der Borgh,
55 2008; Blewett et al., 2010), and are commonly linked to granite intrusion. Marvel Loch deposit (4
56 Moz) within the Southern Cross Greenstone Belt, Western Australia, is an example of major gold-
57 mineralization associated with post compressional, extension-related strike and normal slip
58
59
60
61
62
63
64
65

1 movement. Some gold mineralization is hosted in veins developed during NNW-SSE directed
2 shortening coupled with preferential alteration of a primary gabbro by albite-arsenopyrite-
3 associated gold mineralization that post-dates peak metamorphic, calc-silicate assemblages. The
4 most significant gold mineralization is, however, in vein quartz developed at intersections with NW
5 and N-S trending structures that concentrated veins during NE-SW extension (Nugus, 1999; Witt
6 2000).
7
8
9

10
11
12 Warren et al. (2015) found that at the Castle Hill gold camp, Coolgarde domain, W. Australia, both
13 granite intrusion and later gold mineralization was localized by a bend in the Kunanalling Shear
14 Zone, and that gold mineralization occurred in localized extensional structures during a period of
15 NW-SE compression. They cautioned that local structures may not reflect the regional tectonic
16 picture. This is unlikely to be the case for the Barberton, Geita or Sunrise Dam examples above,
17 where normal components of deformation can be seen on scales of km and cannot therefore be
18 considered as local deformation effects.
19
20
21
22
23
24
25
26
27

28 Present day and recent tectonics in accretionary and collisional orogens may give some useful
29 insights. Accretionary orogens can be divided into advancing and retreating types (Royden, 1993;
30 Cawood and Buchan, 2007). Where the velocity of slab retreat (rollback) is less than that of the
31 overriding plate, advancing orogens are created, characterized by shortening and uplift: this
32 situation arises due to coupling between the subducting and overriding plates, which can be due to
33 flat slab subduction, terrane accretion, or global plate reorganization. Today's eastern Pacific
34 margin orogens are of this type. Where slab retreat is more rapid than the velocity of the overriding
35 plate, extension occurs in the overriding plate, as seen in most Western pacific margins today.
36 Tectonic switching between advancing and retreating modes can occur: for example, the Lachlan
37 fold belt in SE Australia was in long-term retreat mode, punctuated by episodic advancing
38 orogenesis (Collins, 2002). Most orogens probably involve oblique motions in addition to
39 convergence or divergence (Cawood et al., 2009). Collisional orogenies may undergo extension
40 following crustal thickening (e.g. Platt and Vissers, 1989) or as a possible consequence of slab
41 break-off and asthenospheric upwelling (Davies and von Blanckenburg, 1995).
42
43
44
45
46
47
48
49
50
51
52
53
54
55
56

57 Figure 12 shows in situ stress states in the Asia region, encompassing the collisional orogeny of the
58 Himalayas, the intracontinental deformation of the Himalayan hinterland, and the accretionary
59 orogens of the Sumatra-Indonesian and Philippine arcs (Heidbach et al., 2008). It is striking that all
60
61
62
63
64
65

of these tectonic settings show a variety of stress states, commonly in close proximity, especially along the arcs. In a total of 3688 stress determinations, normal and strike slip stresses together (53%) amount to more than reverse stress measurements, even in these archetypal convergent settings. The documentation of gold deposits with extensional or strike-slip tectonics on a greater than local scale suggests that gold deposits can form in several possible stress states and tectonic situations. Such a variety of stress states is also more compatible with known conditions in both accretionary and collisional orogens. An important insight from the case studies above is that structural controls on gold deposits may reflect regional tectonic settings, or they may have quite different local tectonics. It is inadvisable either to infer a regional picture from a deposit scale analysis, or, visa versa, to infer likely deposit scale tectonics from a regional context.

Workflow

The suggested workflow (Fig. 13) includes the main methods used in structural analysis of gold deposits, arranged in order of a classic structural geology approach. However, we wish to emphasise that this is not a prescription. Some methods suggested may be simply inapplicable e.g. if core is not available. The following brief comments on the workflow are mainly intended to give examples and indicate some useful resources.

Data Acquisition

In the context of mapping for structural analysis of gold deposits, it is especially important to focus on lithology and alteration, because of their significance for rheology and fluid flow (e.g. Kisters et al., 2000) in addition to the usual mapping of contacts, fabrics and deformation zones. It is worth spending a significant amount of time to define a consistent lithostratigraphy, for which cores may be the best resource since they provide continuous material that is commonly fresh.

Even the most fragmentary and weathered outcrop can be invaluable in regions of poor outcrop. There is commonly a good case for mapping on several different scales because outcrops can vary from complete, e.g. in three-dimensions underground, to very poor at surface. Drone or Lidar data are invaluable in open pits where access is commonly problematic, and underground where such data is also being increasingly acquired for safety reasons. In most production-orientated situations it is important to map at frequent intervals as pits and stopes advance rapidly.

Core analysis is commonly vital for evaluating structures and their variation in 3D (Vearncombe and Vearncombe, 1998; Marjoribanks, 2010; Holcombe, 2016). Lineations of any type can be

essential clues to directions of increased permeability, but are commonly overlooked in core logging, perhaps because of lack of familiarity with measuring techniques. One of the benefits of working with cores is the complete 3D exposure offered by a core, in which case it is also quite straightforward to look for planes of maximum asymmetry, which will be perpendicular to vorticity vectors: these too can be measured as lines (Blenkinsop et al., 2015). It is greatly preferable to work with whole core because of the greater sampling volume, and therefore to log before core is sampled, even though methods exist for dealing with half core (Blenkinsop and Doyle, 2010).

Microstructural analysis is useful for establishing pressures and temperatures of deformation, overprinting relationships, deformation mechanisms (e.g. Davis et al., 2010), and kinematic analysis (e.g. Blenkinsop and Doyle, 2014; Blenkinsop et al., 2017). It is also invaluable for relating deformation events to mineralization and paragenesis (e.g. Cox et al., 1995; Morey et al., 2007), yet many structural studies of gold mineralization omit this important step (Davis, 2002), perhaps because making and analyzing thin sections adds extra time. However, this time is well spent.

Lithological, structural, geophysical and geochemical data need to be readily visible in relation to each other, and readily viewed at different scales and from different orientations. Such capabilities are inherent in mining software packages, and increasingly in virtual globes such as Google Earth and Worldwind, and now even in GIS packages. Interactive 3D presentations of data are highly effective at communicating complex spatial relationships on all scales: microtomographic images can be combined with outcrop scale photogrammetry (including invaluable drone-acquired imagery; Bemis et al., 2014) and regional 3D models.

Geometric, Kinematic, Dynamic and Rheological Analysis

An accurate 3D geometrical model of structures and mineralization is an essential starting point for kinematic analysis. Geometrical modeling requires input from maps and drilling, and can be done manually or through implicit methods (Cowan et al., 2003; Hill et al., 2014). Structural domains, first introduced at least 60 years ago (Weiss and McIntyre, 1957), are still very useful for understanding spatial and temporal geometrical relationships (Miller and Wilson, 2004b), especially in large, complex ore deposits that are likely to be geometrically, kinematically and dynamically heterogeneous (e.g. Baker et al., 2010). Network geometry can be analyzed from digital data in a semi-automatic way (Healy et al., 2016).

In building a complex deformation chronology based on cross-cutting or overprinting relationships, younging tables are an invaluable way to organize and present data (Angelier, 1991; Potts and Reddy, 2000). Kinematic analysis of deformation zones in multiple orientations is well established for fault zones (Marrett and Allmendinger, 1990), but the same techniques can also be applied to mineralized shear zones (Blenkinsop and Doyle, 2014).

There are many methods available for dynamic or paleostress analysis, which mainly differ in the extent to which different stress tensors can be separated from the data. For single stress states, the following are among some of the most recent: Lisle, (1988); Delvaux, (2012); Thakur et al., (2017). For separating multiple stress states, see the following: Yamaji et al., (2010); Hansen et al., (2015); Lisle and Vandycke, (1996); Lisle and Orife, (2002); Liesa and Lisle, (2004); Shan and Fry, (2005); Žalohar and Vrabec, (2007). There are some interesting methods that combine kinematic and dynamic approaches (e.g. Žalohar and Vrabec, 2008, 2010; Hansen, 2013). None of these methods deal with absolute stress or directly with pore fluid pressures. Fluid inclusion studies are very important for the latter (e.g. Boullier and Robert, 1992b; Robert et al., 1995).

Rheological analysis of gold mineralization ideally relates stress to strain or strain rate over a range of time scales from the seconds of earthquake rupture to the thousands to tens of thousands of years required to form an ore deposit as discussed above. The best numerical modeling will be able to explore these aspects of deformation constrained by realistic rock properties and kinematic or dynamic boundary conditions determined from structural analysis (Schaubs and Zhao, 2002; Schaubs et al., 2006; Mclellan et al., 2007; Potma et al., 2008). However, a major challenge to mechanical modeling in the context of mineral resources is to be able to combine discontinuous and continuous styles of deformation at a variety of scales. In particular, microcracking and brecciation are very difficult to model satisfactorily. The influence of chemical changes on mechanical properties is another level of complexity that is rarely achieved.

Synthesis

An ideal synthesis to conclude the workflow would consist of a geological history in which each deformation event is understood from geometrical, kinematic, dynamic, and rheological view points, and gold mineralization can be tied to one or more specific points in this history. This

requires integrating the classic structural geology approach with geochemistry, geophysics and above all geochronology. Such a synthesis, combined with a good understanding of regional geology, has very powerful predictive capacity. It is not surprising that large ore deposits can be the subject of several or even many PhD studies, given this preferred end point, and nor is it surprising that there is a continual search for magic bullets that can short-cut the workflow.

Conclusions

Hydrothermal gold deposits have several characteristic features, including strong structural control via deformation-induced permeability related to deformation zone networks, fluid-rock interaction resulting in a zoned pattern of alteration, and evidence for a protracted sequence of deformation with cyclic changes in stress and fluid flow. The syn-mineralization kinematics of deposits as a group is truly variable, from pure reverse to pure normal senses of movement on deformation zones. Structural controls on these deposits are one of their most distinctive features.

Geometrical analysis of structures, networks and ore bodies is the most basic step in analyzing hydrothermal gold deposits. Geometrical analysis can now include new techniques of analyzing network topology, as well as a more quantitative approach to relating ore body geometry to deformation. Kinematic analysis is also essential for the latter purpose, as well as to relate deposit-scale features to regional tectonics. Several examples show that it is important to move beyond the Ramsay and Graham simple shear paradigm for shear zone kinematics; inclusion of significant pure shear components in deformation zones can change relationships between ore bodies, lineations, and vorticity vectors, and this is crucial for predicting ore body geometry and in numerical mechanical modeling. An appreciation that many deformation zone networks are polygonal, which is to be expected in a general state of strain, may also be important because of their influence on fluid pathways.

A dynamic analysis of hydrothermal gold deposits will assess pore fluid pressure and stress, preferably using numerical mechanical models. The involvement of fluids in slow slip, and the scale of slip increments in vein textures, suggests that slow slip is likely to be involved in mineralization. Numerical mechanical models have considerable predictive power, but they do not yet successfully encompass the likely range of slip speeds on faults, nor deal effectively with cyclic behavior or the complexity of overprinting that obscures early dynamic behavior.

1 Analysis of rheology is the key in many cases to understanding the structural controls on ore bodies,
2 which are commonly located on rheological boundaries. Reactivation and multiple cycles of
3 mineralization, sometimes separated by tens to hundreds of millions of years, is a feature of many
4 deposits, including some of the largest. If inherited structures are weaker than intact rock, they can
5 be reactivated in a variety of orientations. Slip and dilation tendency are useful techniques for
6 analyzing propensity for reactivation.
7
8
9
10

11
12
13
14
15 Stress states in all types of orogenic zones observed today are variable throughout the crust. A
16 logical implication is that hydrothermal gold deposits formed and exhumed from previous orogenies
17 will record a complex structural history. Unraveling that history, by breaking it down into each
18 separate phase, is a traditional structural geology approach that is still essential in order to work out
19 which phase or phases of deformation are associated with mineralization. Short time-scale stress
20 changes associated with seismic or sub-seismic cycles within the same phase of deformation need to
21 be distinguished from longer time scale switches in tectonic mode. Short time scale, cyclic changes
22 are likely to be represented by numerous repetitions and mutually cross-cutting relationships
23 between fault zones, veins and shear zones; longer time-scale tectonic switches will show a
24 consistent structural paragenesis. There may be great variation in the scale over which a tectonic
25 setting applies, and there may be rapid temporal changes, so that it is inadvisable to infer local
26 tectonics from regional patterns, and visa versa.
27
28
29
30
31
32
33
34
35
36
37
38
39

40 New developments in structural geology that appear to have great promise for understanding gold
41 deposit genesis and for exploration include the application of network and percolation theories, and
42 non-equilibrium thermodynamics. The latter is a quantifiable systems approach, which integrates
43 deformation (in the sense of displacements and strain), stress, fluids, heat and chemical reactions.
44 The non-linear behavior of an ore-forming system leads to multifractal properties that can be
45 measured and should have direct exploration implications. Even these characteristics, however, will
46 need to be placed in a complete structural history.
47
48
49
50
51
52
53
54
55
56

57 **Acknowledgements**

58

59 Discussions with Tim Baker, James Cleverley, Simon Dominy, Mark Doyle, John McLellan,
60 Howard Poulsen and Dave Sanderson were helpful in developing some of the ideas in this article.
61
62
63
64
65

Other formative influences were Bruce Hobbs, Alex Kisters, Alison Ord, Rick Sibson, Basil Tikoff, Julian Vearncombe and Steve Wojtal, though they do not necessarily endorse the contents. We are grateful to Geof Steed, and reviewers Howard Poulsen, Tim Baker and Steve Micklethwaite for helpful comments, and editor Julie Rowland for advice.

References

- Allibone, A., Teasdale, J., Cameron, G., Etheridge, M., Uttley, P., Soboh, A., Appiah-Kubi, J., Adanu, A., Arthur, R., Mamphey, J., Odoom, B., Zuta, J., Tsikata, A., Pataye, F., Famiyeh, S., 2002a. Timing and structural controls on gold mineralization at the Bogoso mine, Ghana, West Africa. *Econ. Geol.* 97-5, 949-, 949–969.
- Allibone, A.H., McCuaig, T.C., Harris, D., Etheridge, M., Munroe, S., Byrne, D., 2002b. Chapter 4 Structural Controls on Gold Mineralization at the Ashanti Gold Deposit, Obuasi, Ghana. *Soc. Econ. Geol. Spec. Publ.* 9, 65–93.
- Anderson, E.M., 1905. The dynamics of faulting. *Trans. Edinburgh Geol. Soc.* 8, 387–402. doi:10.1144/transed.8.3.387
- Angelier, J., 1975. Sur l'analyse de mesures recueillies sans des sites faillés: l'utilité d'une confrontation entre les méthodes dynamiques et cinématiques. *Comptes Rendus l'Académie des Sci. Paris D218*, 1805–1808.
- Angelier, J., 1991. Analyse chronologique matricielle et succession régionale des événements tectoniques. *Comptes rendus l'Académie des Sci. Série 2, Mécanique, Phys. Chim. Sci. l'univers, Sci. la Terre* 312, 1633–1638.
- Arne, D.C., Bierlin, F.P., Morgan, J.W., Stein, H.J., 2001. Re-Os dating of sulfides associated with gold mineralization in Central Victoria, Australia. *Econ. Geol.* doi:10.2113/gsecongeo.96.6.1455
- Baker, T., Bertelli, M., Blenkinsop, T., Cleverly, J., McLellan, J.G., Nugus, M., Gillen, D., 2010. PTX conditions of fluids in the Sunrise Dam gold deposit, Western Australia, and implications for the interplay between deformation and fluids. *Econ. Geol.* 105, 873–894.
- Barnhoorn, A., Cox, S.F., Robinson, D.J., Senden, T., 2010. Stress- and fluid-driven failure during fracture array growth: Implications for coupled deformation and fluid flow in the crust. *Geology* 38, 779–782. doi:10.1130/G31010.1
- Bateman, R., Hagemann, S., 2004. Gold mineralisation throughout about 45 Ma of Archaean

orogenesis: Protracted flux of gold in the Golden Mile, Yilgarn craton, Western Australia.
Miner. Depos. 39, 536–559. doi:10.1007/s00126-004-0431-2

Bemis, S.P., Micklethwaite, S., Turner, D., James, M.R., Akciz, S., T. Thiele, S., Bangash, H.A.,
2014. Ground-based and UAV-Based photogrammetry: A multi-scale, high-resolution
mapping tool for structural geology and paleoseismology. J. Struct. Geol. 69, 163–178.
doi:10.1016/j.jsg.2014.10.007

Ben-zion, Y., 2008. Collective Behavior of Earthquakes and Faults. Rev. Geophys. 46, 1–70.
doi:10.1029/2008RG000260

Beroza, G.C., Ide, S., 2011. Slow Earthquakes and Nonvolcanic Tremor. Annu. Rev. Earth Planet.
Sci. 39, 271–296. doi:10.1146/annurev-earth-040809-152531

Bierlein, F.P., Maher, S., 2001. Orogenic disseminated gold in phanerozoic fold belts - Examples
from Victoria, Australia and elsewhere. Ore Geol. Rev. 18, 113–148. doi:10.1016/S0169-
1368(01)00019-1

Bierlein, F.P., Groves, D.I., Goldfarb, R.J., Dubé, B., 2006. Lithospheric controls on the formation
of provinces hosting giant orogenic gold deposits. Miner. Depos. 40, 874–886.
doi:10.1007/s00126-005-0046-2

Blenkinsop, T.G., 2004a. Orebody geometry in lode gold deposits from Zimbabwe: implications for
fluid flow, deformation and mineralization. J. Struct. Geol. 26, 1293–1301.
doi:10.1016/j.jsg.2003.11.010

Blenkinsop, T.G., 2004b. Pure and Simple: A Practical Guide to Predicting Ore Body Geometry in
Shear Zones, in: Dominy, S.C. (Ed.), Mining and Resource Geology Symposium. EGRU,
James Cook University, Townsville, pp. 9–18.

Blenkinsop, T., 2014. Scaling Laws for the Distribution of Gold, Geothermal, and Gas Resources.
Pure Appl. Geophys. 2045–2056. doi:10.1007/s00024-014-0909-5

Blenkinsop, T.G., Frei, R., 1996. Archean and proterozoic mineralization and tectonics at the Renco
mine (Northern Marginal Zone, Limpopo Belt, Zimbabwe). Econ. Geol. 91, 1225–1238.
doi:10.2113/gsecongeo.91.7.1225

Blenkinsop, T.G., Kadzvi, S., 2006. Fluid flow in shear zones: insights from the geometry and
evolution of ore bodies at Renco gold mine, Zimbabwe. Geofluids 6, 334–345.

Blenkinsop, T.G., Doyle, M.G., 2010. A method for measuring the orientations of planar structures
in cut core. J. Struct. Geol. 32, 741–745. doi:10.1016/j.jsg.2010.04.011

Blenkinsop, T.G., Doyle, M.G., 2014. Structural controls on gold mineralization on the margin of

the Yilgarn craton, Albany–Fraser orogen: The Tropicana deposit, Western Australia. *J. Struct. Geol.* 67, 189–204. doi:10.1016/j.jsg.2014.01.013

Blenkinsop, T.G., Schmidt Mumm, A., Kumi, R., Sangmor, S., 1994. Structural geology of the Ashanti gold mine. *Geol. Jahrb. D* 100, 131–153.

Blenkinsop, T.G., Oberthür, T., Mapeto, O., 2000. Gold mineralization in the Mazowe area, Harare–Bindura–Shamva greenstone belt, Zimbabwe: I. Tectonic controls on mineralization. *Miner. Depos.* 35, 126–137. doi:10.1007/s001260050011

Blenkinsop, T., Kröner, A., Chiwara, V., 2004. Single stage, late Archaean exhumation of granulites in the Northern Marginal Zone, Limpopo Belt, Zimbabwe, and relevance to gold mineralization at Renco mine. *South African J. Geol.* 107, 377–396.

Blenkinsop, T., Kreuzer, O.P., Mclellan, J., Baker, T., 2009. Sunrise Dam Gold Mine , Western Australia : Mechanical Controls on an Archean Lode Gold Hydrothermal System, in: Williams, P.J. (Ed.), *Proceedings of the Tenth Biennial SGA Meeting*. Australian Institute of Mining and Metallurgy, Townsville, pp. 800–802.

Blenkinsop, T.G., Doyle, M., Nugus, M., 2015. A unified approach to measuring structures in orientated drill core, in: Richards, F. L., Richardson, N. J., Rippington, S. J., Wilson, R. W. & Bond, C. E. (Eds) *Industrial Structural Geology: Principles, Techniques and Integration*. Geological Society, London, Special Publications, 421, <http://dx.doi.org/10.1144/SP421.1>. doi:10.1144/SP421.1

Blenkinsop, T., Tripp, G., Gillen, D., 2018. The relation between mineralization and tectonics at the Kainantu gold-copper deposit, Papua New Guinea. *Spec. Publ. Geol. Soc.* 453.

Blewett, R.S., Czarnota, K., Henson, P.A., 2010. Structural-event framework for the eastern Yilgarn Craton, Western Australia, and its implications for orogenic gold. *Precambrian Res.* 183, 203–229. doi:<http://dx.doi.org/10.1016/j.precamres.2010.04.004>

Bons, P.D., 2001. The formation of large quartz veins by rapid ascent of fluids in mobile hydrofractures. *Tectonophysics* 336, 1–17. doi:[http://dx.doi.org/10.1016/S0040-1951\(01\)00090-7](http://dx.doi.org/10.1016/S0040-1951(01)00090-7)

Bottrell, S.H., Shepherd, T.J., Yardley, B.W.D., Dubessy, J., 1988. Fluid Inclusion Model for the Genesis of the Ores of the Dalgellau Gold Belt, North Wales. *J. Geol. Soc. London* 145, 139–145.

Boullier, A.-M., Robert, F., 1992. Palaeoseismic events recorded in Archaean gold-quartz vein networks, Val d’Or, Abitibi, Quebec, Canada. *J. Struct. Geol.* 14, 161–179.

- Brace, W.F., 1980. Permeability of crystalline and argillaceous rocks. *Int. J. Rock Mech. Min. Sci. Geomech. Abstr.* 17, 241–251. doi:10.1016/0148-9062(80)90807-4
- Calais, E., d'Oreye, N., Albaric, J., Deschamps, A., Delvaux, D., Déverchère, J., Ebinger, C., Ferdinand, R.W., Kervyn, F., Macheyeki, A.S., Oyen, A., Perrot, J., Saria, E., Smets, B., Stamps, D.S., Wauthier, C., 2008. Strain accommodation by slow slip and dyking in a youthful continental rift, East Africa. *Nature* 456, 783–787. doi:10.1038/nature07478
- Carvell, J., Blenkinsop, T., Clarke, G., Tonelli, M., 2014. Scaling, kinematics and evolution of a polymodal fault system: Hail Creek Mine, NE Australia. *Tectonophysics* 632, 138–150. doi:10.1016/j.tecto.2014.06.003
- Cawood, P.A., Buchan, C., 2007. Linking accretionary orogenesis with supercontinent assembly. *Earth- Sci. Rev.* 82, 217–256.
- Cawood, P.A., Kroner, A., Collins, W.J., Kusky, T.M., Mooney, W.D., Windley, B.F., 2009. Accretionary orogens through Earth history. *Geol. Soc. London, Spec. Publ.* 318, 1–36. doi:10.1144/SP318.1
- Chamberlain, C.J., Shelly, D.R., Townend, J., Stern, T., 2014. Low-frequency earthquakes reveal punctuated slow slip on the deep extent of the Alpine Fault, New Zealand. *Geochemistry, Geophys. Geosystems* n/a-n/a. doi:10.1002/2014GC005436
- Chang, C., Haimson, B., 2012. A Failure Criterion for Rocks Based on True Triaxial Testing. *Rock Mech. Rock Eng.* 45, 1007–1010. doi:10.1007/s00603-012-0280-8
- Choukroune, P., Gapais, D., 1983. Strain Patterns in Rocks Strain pattern in the Aar Granite (Central Alps): Orthogneiss developed by bulk inhomogeneous flattening. *J. Struct. Geol.* 5, 411–418. doi:[http://dx.doi.org/10.1016/0191-8141\(83\)90027-5](http://dx.doi.org/10.1016/0191-8141(83)90027-5)
- Collins, W.J., 2002. Hot orogens, tectonic switching, and creation of the continental crust. *Geology* 30, 535–538.
- Colvine, A.C., 1989. An empirical model for the formation of Archean gold deposits: products of final cratonization of the Superior Province, Canada. *Econ. Geol. Monogr.* 6, 37–53.
- Cowan, E.J., Beatson, R.K., Ross, H.J., Fright, W.R., McLennan, T.J., Evans, T.R., Carr, J.C., Lane, R.G., Bright, D. V, Gillman, A.J., 2003. Practical implicit geological modelling, in: Fifth International Mining Geology Conference. Australian Institute of Mining and Metallurgy Bendigo, Victoria, pp. 17–19.
- Cox, S.F., 1999. Deformational controls on the dynamics of fluid flow in mesothermal gold

systems. Geol. Soc. London, Spec. Publ. 155, 123–140. doi:10.1144/GSL.SP.1999.155.01.10

- Cox, S.F., Ruming, K., 2004. The St Ives mesothermal gold system, Western Australia—a case of golden aftershocks? *J. Struct. Geol.* 26, 1109–1125.
doi:http://dx.doi.org/10.1016/j.jsg.2003.11.025
- Cox, S.F., Sun, S.S., Etheridge, M.A., Wall, V.J., Potter, T.F., 1995. Structural and geochemical controls on the development of turbidite-hosted gold quartz vein deposits, Wattle Gully mine, central Victoria, Australia. *Econ. Geol.* 90, 1722–1746.
- Craw, D., Windle, S.J., Angus, P. V., 1999. Gold mineralization without quartz veins in a ductile-brittle shear zone, Macraes Mine, Otago Schist, New Zealand. *Miner. Depos.* 34, 382–394.
doi:10.1007/s001260050211
- Czarnota, K., Blewett, R.S., Champion, D.C., Henson, P.A., Cassidy, K.F., 2007. Significance of extensional tectonics in orogenic gold systems: an example from the Eastern Goldfields Superterrane, Yilgarn Craton, Australia, *Digging Deeper*, Vols 1 and 2: *Digging Deeper*.
- Czarnota, K., Blewett, R.S., Goscombe, B., 2010. Predictive mineral discovery in the eastern Yilgarn Craton, Western Australia: An example of district scale targeting of an orogenic gold mineral system. *Precambrian Res.* 183, 356–377. doi:10.1016/j.precamres.2010.08.014
- Davies, H., von Blanckenburg, F., 1995. Slab breakoff: A model of lithosphere detachment and its test in the magmatism and deformation of collisional orogens. *Earth Planet. Sci. Lett.* 129, 85–102. doi:10.1016/0012-821X(94)00237-S
- Davis, B.K., 2002. *Applied Structural Geology for Exploration and Mining*. Aust. Inst. Geosci. Bull. 36, 242.
- Davis, B.K., Maidens, E., 2003. Archaean orogen-parallel extension: Evidence from the northern Eastern Goldfields Province, Yilgarn Craton, in: *Precambrian Research*. pp. 229–248.
- Davis, B.K., Blewett, R.S., Squire, R., Champion, D.C., Henson, P. a., 2010a. Granite-cored domes and gold mineralisation: Architectural and geodynamic controls around the Archaean Scotia-Kanowna Dome, Kalgoorlie Terrane, Western Australia. *Precambrian Res.* 183, 316–337.
doi:10.1016/j.precamres.2010.01.011
- Davis, B.K., Blewett, R.S., Squire, R., Champion, D.C., Henson, P. a., 2010b. Granite-cored domes and gold mineralisation: Architectural and geodynamic controls around the Archaean Scotia-Kanowna Dome, Kalgoorlie Terrane, Western Australia. *Precambrian Res.* 183, 316–337.
doi:10.1016/j.precamres.2010.01.011

- Delvaux, D., 2012. Release of program Win-Tensor 4.0 for tectonic stress inversion: statistical expression of stress parameters, in: *Geophysical Research Abstracts*.
- Dipple, G.M., Ferry, J.M., 1992. Metasomatism and fluid flow in ductile fault zones. *Contrib. to Mineral. Petrol.* 112, 149–164. doi:10.1007/BF00310451
- Dirks, P.H.G.M., Charlesworth, E.G., Munyai, M.R., 2009. Cratonic extension and Archaean gold mineralisation in the Sheba-Fairview mine, Barberton Greenstone Belt, South Africa. *South African J. Geol.* 112, 291–316.
- Dirks, P.H.G.M., Charlesworth, E.G., Munyai, M.R., Wormald, R., 2013. Stress analysis, post-orogenic extension and 3.01Ga gold mineralisation in the Barberton Greenstone Belt, South Africa. *Precambrian Res.* 226, 157–184. doi:10.1016/j.precamres.2012.12.007
- Dominy, S.C., Phelps, R.F.G., Camm, G.S., 1996a. Geological controls on gold grade distribution in Chidlaw link zone, Gwynfynydd mine, Dolgellau, north Wales. *Trans. Inst. Min. Metall. Sect. B. Appl. Earth Sci.* 105, B151.
- Dominy, S.C., Phelps, R.F.G., Guard, C.L., 1996b. Geology and exploitation of complex gold-bearing veins in the Gwynfynydd mine, Dolgellau, North Wales, U.K. *Br. Min.* 57, 70–91.
- Dube, B., Poulsen, H., Guha, J., 1989. The effects of layer anisotropy on auriferous shear zones; the Norbeau Mine, Quebec. *Econ. Geol.* 84, 871–878. doi:10.2113/gsecongeo.84.4.871
- Eisenlohr, B.N., Groves, D., Partington, G.A., 1989. Crustal-scale shear zones and their significance to Archaean gold mineralization in Western Australia. *Miner. Depos.* 24, 1–8. doi:10.1007/BF00206714
- Fagereng, A., Sibson, R.H., 2010. Melange rheology and seismic style. *Geology* 38, 751–754. doi:10.1130/G30868.1
- Fagereng, Å., Remitti, F., Sibson, R.H., 2011. Incrementally developed slickenfibers — Geological record of repeating low stress-drop seismic events? *Tectonophysics* 510, 381–386. doi:http://dx.doi.org/10.1016/j.tecto.2011.08.015
- Farrell, N.J.C., Healy, D., Taylor, C.W., 2014. Anisotropy of permeability in faulted porous sandstones. *J. Struct. Geol.* 63, 50–67. doi:10.1016/j.jsg.2014.02.008
- Ford, A., Blenkinsop, T., McLellan, J., 2009. Factors affecting fluid flow in strike-slip fault systems: coupled deformation and fluid flow modelling with application to the western Mount Isa Inlier, Australia. *Geofluids* 1–22. doi:10.1111/j.1468-8123.2008.00219.x
- Fossen, H., 1993. The deformation matrix for simultaneous simple shearing, pure shearing and volume change, and its application to transpression-transtension tectonics. *J. Struct. Geol.* 15,

- Fyfe, W.S., Kerrich, R., 1976. Geochemical prospecting: Extensive versus intensive factors. *J. Geochemical Explor.* 6, 177–192.
- Gapais, D., Bale, P., Choukroune, P., Cobbold, P., Mahjoub, Y., Marquer, D., 1987. Shear Criteria in Rocks Bulk kinematics from shear zone patterns: some field examples. *J. Struct. Geol.* 9, 635–646. doi:[http://dx.doi.org/10.1016/0191-8141\(87\)90148-9](http://dx.doi.org/10.1016/0191-8141(87)90148-9)
- Goldfarb, R.J., Groves, D.I., Gardoll, S., 2001. Orogenic gold and geologic time: a global synthesis. *Ore Geol. Rev.* 18, 1–75. doi:[http://dx.doi.org/10.1016/S0169-1368\(01\)00016-6](http://dx.doi.org/10.1016/S0169-1368(01)00016-6)
- Goldfarb, R.J., Baker, T., Dube, B., Groves, D.I., Hart, C.J., Gosselin, P., 2005. Distribution, character, and genesis of gold deposits in metamorphic terranes. *Econ. Geol.* 100th Anni.
- Gomberg, J., 2010. Slow-slip phenomena in Cascadia from 2007 and beyond: A review. *Geol. Soc. Am. Bull.* 122, 963–978. doi:10.1130/B30287.1
- Groves, D., Phillips, G., 1987. The genesis and tectonic control on Archaean gold deposits of the western Australian shield—a metamorphic replacement model. *Ore Geol. Rev.* 2, 287–322. doi:10.1016/0169-1368(87)90009-6
- Groves, D.I., Goldfarb, R.J., Gebre-Mariam, M., Hagemann, S.G., Robert, F., 1998. Orogenic gold deposits: A proposed classification in the context of their crustal distribution and relationship to other gold deposit types. *Ore Geol. Rev.* 13, 7–27. doi:[http://dx.doi.org/10.1016/S0169-1368\(97\)00012-7](http://dx.doi.org/10.1016/S0169-1368(97)00012-7)
- Groves, D., Goldfarb, R., Robert, F., Hart, C., 2003. Gold Deposits in Metamorphic Belts : Overview of Current Understanding , Outstanding Problems , Future Research , and Exploration Significance. *Econ. Geol.* 98, 1–29.
- Gustafson, L.B., 1989. SEG distinguished lecture in applied geology the importance of structural analysis in gold exploration. *Econ. Geol.* 84, 987–993. doi:10.2113/gsecongeo.84.4.987
- Hansen, J.-A., 2013. Direct inversion of stress, strain or strain rate including vorticity: A linear method of homogenous fault–slip data inversion independent of adopted hypothesis. *J. Struct. Geol.* 51, 3–13. doi:10.1016/j.jsg.2013.03.014
- Hansen, J.-A., Bergh, S.G., Osmundsen, P.T., Redfield, T.F., 2015. Stress inversion of heterogeneous fault-slip data with unknown slip sense: An objective function algorithm contouring method. *J. Struct. Geol.* 70, 119–140. doi:10.1016/j.jsg.2014.11.005
- Healy, D., Blenkinsop, T.G., Timms, N.E., Meredith, P.G., Mitchell, T.M., Cooke, M.L., 2015. Polymodal faulting: Time for a new angle on shear failure. *J. Struct. Geol.* 80, 57–71.

doi:10.1016/j.jsg.2015.08.013

- 1 Healy, D., Rizzo, R.E., Cornwell, D.G., Farrell, N.J.C., Watkins, H., Timms, N.E., Gomez-Rivas,
2 E., Smith, M., 2016. FracPaQ: A MATLABTM toolbox for the quantification of fracture
3 patterns. *J. Struct. Geol.* 95, 1–16. doi:10.1016/j.jsg.2016.12.003
4
5
6
7 Heard, H.C., 1960. Transition from Brittle Fracture to Ductile Flow in Solenhofen Limestone as a
8 Function of Temperature, Confining Pressure, and Interstitial Fluid Pressure, in: *Geological*
9 *Society of America Memoir 79*. Geological Society of America, pp. 193–226.
10
11
12
13 doi:10.1130/MEM79-p193
14
15 Heidbach, O., Tingay, M., Barth, A., Reinecker, J., Kurfeß, D., Müller, B., 2008. The World Stress
16 Map database release 2008. doi:10.1594/GFZ.WSM.Rel2008
17
18
19 Hill, E.J., Oliver, N.H.S., Cleverley, J.S., Nugus, M.J., Carswell, J., Clark, F., 2014.
20
21 Characterisation and 3D modelling of a nuggety, vein-hosted gold ore body, Sunrise Dam,
22 Western Australia. *J. Struct. Geol.* 67, 222–234. doi:10.1016/j.jsg.2013.10.013
23
24
25 Hobbs, B., Ord, A., Gorczyk, W., Gessner, K., 2012. Nonlinear and non-equilibrium
26 thermodynamics without the complex mathematics by 1–53.
27
28
29 Hodgson, C.J., 1989. Patterns of Mineralization, in: Bursnall, J.T. (Ed.), *Mineralization and Shear*
30 *Zones: Short Course Notes Volume 6*. Geological Association of Canada, Montreal, pp. 51–88.
31
32
33 Holcombe, R.J., 2016. Mapping and structural geology in mineral exploration: where theory hits the
34 fan. *HCOV Global*.
35
36
37
38 Holyland, P.W., Ojala, V.J., 1997. Computer-aided structural targeting in mineral exploration: Two-
39
40 and three-dimensional stress mapping. *Aust. J. Earth Sci.* 44, 421–432.
41
42
43 doi:10.1080/08120099708728323
44
45 Hou, Z., Cook, N.J., 2009. Metallogensis of the Tibetan collisional orogen: A review and
46 introduction to the special issue. *Ore Geol. Rev.* 36, 2–24.
47
48
49 doi:10.1016/j.oregeorev.2009.05.001
50
51
52 Hudleston, P., 1999. Strain compatibility and shear zones: is there a problem? *J. Struct. Geol.* 21,
53 923–932. doi:http://dx.doi.org/10.1016/S0191-8141(99)00060-7
54
55
56 Ingebritsen, S.E., Manning, C.E., 2010. Permeability of the continental crust : dynamic variations
57 inferred from seismicity and metamorphism. *Geofluids* 10, 193–205. doi:10.1111/j.1468-
58 8123.2010.00278.x
59
60
61
62 Jelsma, H.A., Huizenga, J.M., Touret, J.L.R., 1998. Fluids and epigenetic gold mineralization at
63
64
65

Shamva Mine, Zimbabwe: a combined structural and fluid inclusion study. *J. African Earth Sci.* 27, 55–70.

Jia, Y., Kerrich, R., 2000. Giant quartz vein systems in accretionary orogenic belts : the evidence for a metamorphic fluid origin from N 15 N and N 13 C studies. *Earth Planet. Sci. Lett.* 184, 211–224.

Jiang, D., Williams, P.F., 1998. High-strain zones: a unified model. *J. Struct. Geol.* 20, 1105–1120. doi:[http://dx.doi.org/10.1016/S0191-8141\(98\)00025-X](http://dx.doi.org/10.1016/S0191-8141(98)00025-X)

Jolivet, R., Candela, T., Lasserre, C., Renard, F., Klinger, Y., Doin, M.-P., 2014. The Burst-Like Behavior of Aseismic Slip on a Rough Fault: The Creeping Section of the Haiyuan Fault, China. *Bull. Seismol. Soc. Am.* 105, 480–488. doi:10.1785/0120140237

Jones, R.R., Holdsworth, R.E., 1998. Oblique simple shear in transpression zones. *Geol. Soc. London, Spec. Publ.* 135, 35–40. doi:10.1144/GSL.SP.1998.135.01.03

Kirschner, D.L., Teixell, a., 1996. Three-dimensional geometry of kink bands in slates and its relationship with finite strain. *Tectonophysics* 262, 195–211. doi:10.1016/0040-1951(96)00003-0

Kisters, A.F.M., Kolb, J., Meyer, F.M., 1998. Gold mineralization in high-grade metamorphic shear zones of the Renco Mine, southern Zimbabwe. *Econ. Geol.* 93, 587–601. doi:10.2113/gsecongeo.93.5.587

Kisters, A.F., Kolb, J., Meyer, F.M., Hoernes, S., 2000. Hydrologic segmentation of high-temperature shear zones: structural, geochemical and isotopic evidence from auriferous mylonites of the Renco mine, Zimbabwe. *J. Struct. Geol.* 22, 811–829. doi:10.1016/S0191-8141(00)00006-7

Kokelaar, P., 1988. Tectonic controls of Ordovician arc and marginal basin volcanism in Wales. *J. Geol. Soc. London.* 145, 759–775. doi:10.1144/gsjgs.145.5.0759

Kolb, J., Kisters, A., Hoernes, S., Meyer, F., 2000. The origin of fluids and nature of fluid–rock interaction in mid-crustal auriferous mylonites of the Renco mine, southern Zimbabwe. *Miner. Depos.* 35, 109–125.

Krantz, R.W., 1988. Multiple fault sets and three-dimensional strain: Theory and application. *J. Struct. Geol.* 10, 225–237. doi:10.1016/0191-8141(88)90056-9

Kruckenberger, S.C., Ferré, E.C., Teyssier, C., Vanderhaeghe, O., Whitney, D.L., Seaton, N.C.A., Skord, J.A., 2010. Viscoplastic flow in migmatites deduced from fabric anisotropy: An example from the Naxos dome, Greece. *J. Geophys. Res. Solid Earth* 115, n/a-n/a.

- Laing, W.P., 2004. Tension vein arrays in progressive strain: complex but predictable architecture, and major hosts of ore deposits. *J. Struct. Geol.* 26, 1303–1315. doi:10.1016/j.jsg.2003.11.006
- Lawn, B., 1993. *Fracture of Brittle Solids*, Cambridge Music Handbooks. Cambridge University Press.
- Lester, D.R., Ord, A., Hobbs, B.E., 2012. The mechanics of hydrothermal systems: II. Fluid mixing and chemical reactions. *Ore Geol. Rev.* 49, 45–71. doi:10.1016/j.oregeorev.2012.08.002
- Liesa, C.L., Lisle, R.J., 2004. Reliability of methods to separate stress tensors from heterogeneous fault-slip data. *J. Struct. Geol.* 26, 559–572. doi:10.1016/j.jsg.2003.08.010
- Lin, A., 2001a. S–C fabrics developed in cataclastic rocks from the Nojima fault zone, Japan and their implications for tectonic history. *J. Struct. Geol.* 23, 1167–1178. doi:10.1016/S0191-8141(00)00171-1
- Lin, S., 2001b. Stratigraphic and structural setting of the Hemlo gold deposit, Ontario, Canada. *Econ. Geol.* 96, 477–507.
- Lin, S., Jiang, D., Williams, P.F., 1998. Transpression (or transtension) zones of triclinic symmetry: natural example and theoretical modelling. *Geol. Soc. London, Spec. Publ.* 135, 41–57. doi:10.1144/GSL.SP.1998.135.01.04
- Lisle, R.J., 1988. ROMSA : A BASIC P R O G R A M FOR PALEOSTRESS ANALYSIS USING FAULT-STRIATION DATA. *Comput. Geosci.* 14, 255–259.
- Lisle, R.J., Vandycke, S., 1996. Separation of multiple stress events by fault striation analysis: an example from Variscan and younger structures at Ogmore, South Wales. *J. Geol. Soc. London.* 153, 945–953. doi:10.1144/gsjgs.153.6.0945
- Lisle, R.J., Orife, T., 2002. STRESSTAT: a Basic program for numerical evaluation of multiple stress inversion results. *Comput. Geosci.* 28, 1037–1040. doi:10.1016/S0098-3004(02)00018-3
- Lisle, R.J., Orife, T.O., Arlegui, L., Liesa, C., Srivastava, D.C., 2006. Favoured states of palaeostress in the Earth's crust: evidence from fault-slip data. *J. Struct. Geol.* 28, 1051–1066. doi:10.1016/j.jsg.2006.03.012
- Manning, C.E., Ingebritsen, S.E., 1999. Permeability of the Continental Crust: Implications of Geothermal Data and Metamorphic Systems. *Rev. Geophys.* 37, 127–150.
- Marjoribanks, R., 2010. Geological methods in mineral exploration and mining, *Geological Methods in Mineral Exploration and Mining*. doi:10.1007/978-3-540-74375-0

- Marrett, R., Allmendinger, R.W., 1990. Kinematic analysis of fault-slip data. *J. Struct. Geol.* 12, 973–986. doi:[http://dx.doi.org/10.1016/0191-8141\(90\)90093-E](http://dx.doi.org/10.1016/0191-8141(90)90093-E)
- McCuaig, T.C., Hronsky, J.M.A., 2016. The mineral system concept: the key to exploration targeting. *Econ. Geol.* 153–175.
- McLellan, J.G., Blenkinsop, T., Nugus, M., Erickson, M., 2007. Numerical simulation of deformation and controls on mineralization at the Sunrise Dam Gold Mine, Western Australia, in: *Proceedings of the Ninth Biennial SGA Meeting*. pp. 1455–1458.
- Micklethwaite, S., Cox, S.F., 2004. Fault-segment rupture, aftershock-zone fluid flow, and mineralization. *Geology* 32, 813. doi:[10.1130/G20559.1](https://doi.org/10.1130/G20559.1)
- Micklethwaite, S., Cox, S., 2006. Progressive fault triggering and fluid flow in aftershock domains: Examples from mineralized Archaean fault systems. *Earth Planet. Sci. Lett.* 250, 318–330. doi:[10.1016/j.epsl.2006.07.050](https://doi.org/10.1016/j.epsl.2006.07.050)
- Micklethwaite, S., Ford, A., Witt, W., Sheldon, H.A., 2015. The where and how of faults, fluids and permeability - insights from fault stepovers, scaling properties and gold mineralisation. *Geofluids* 15, 240–251. doi:[10.1111/gfl.12102](https://doi.org/10.1111/gfl.12102)
- Miller, J.M., Wilson, C.J.L., 2004a. Structural analysis of faults related to a heterogeneous stress history: reconstruction of a dismembered gold deposit, Stawell, western Lachlan Fold Belt, Australia. *J. Struct. Geol.* 26, 1231–1256. doi:[10.1016/j.jsg.2003.11.004](https://doi.org/10.1016/j.jsg.2003.11.004)
- Miller, J.M., Wilson, C.J.L., 2004b. Structural analysis of faults related to a heterogeneous stress history: reconstruction of a dismembered gold deposit, Stawell, western Lachlan Fold Belt, Australia. *J. Struct. Geol.* 26, 1231–1256. doi:[10.1016/j.jsg.2003.11.004](https://doi.org/10.1016/j.jsg.2003.11.004)
- Miller, J., Blewett, R., Tunjic, J., Connors, K., 2010. The role of early formed structures on the development of the world class St Ives Goldfield, Yilgarn, WA. *Precambrian Res.* 183, 292–315. doi:[10.1016/j.precamres.2010.08.002](https://doi.org/10.1016/j.precamres.2010.08.002)
- Mitchell, T.M., Faulkner, D.R., 2008. Experimental measurements of permeability evolution during triaxial compression of initially intact crystalline rocks and implications for fluid flow in fault zones. *J. Geophys. Res. Solid Earth* 113, 1–16. doi:[10.1029/2008JB005588](https://doi.org/10.1029/2008JB005588)
- Mitra, G., 1979. Ductile deformation zones in Blue Ridge basement rocks and estimation of finite strains. *Geol. Soc. Am. Bull.* 90, 935–951. doi:[10.1130/0016-7606\(1979\)90<935:DDZIBR>2.0.CO;2](https://doi.org/10.1130/0016-7606(1979)90<935:DDZIBR>2.0.CO;2)
- Moeck, I., Kwiatek, G., Zimmermann, G., 2009. Slip tendency analysis, fault reactivation potential and induced seismicity in a deep geothermal reservoir. *J. Struct. Geol.* 31, 1174–1182.

- Morelli, R.M., Creaser, R.A., Selby, D., Kontak, D.J., Horne, R.J., 2005. Rhenium-Osmium Geochronology of Arsenopyrite in Meguma Group Gold Deposits, Meguma Terrane, Nova Scotia, Canada: Evidence for Multiple Gold-Mineralizing Events. *Economic Geology*, 100, 1229–1242.
- Morelli, R.M., Bell, C.C., Creaser, R.A., Simonetti, A., 2010. Constraints on the genesis of gold mineralization at the Homestake Gold Deposit, Black Hills, South Dakota from rhenium-osmium sulfide geochronology. *Miner. Depos.* 45, 461–480. doi:10.1007/s00126-010-0284-9
- Morey, A.A., Weinberg, R.F., Bierlein, F.P., 2007. The structural controls of gold mineralisation within the Bardoc Tectonic Zone, Eastern Goldfields Province, Western Australia: Implications for gold endowment in shear systems. *Miner. Depos.* 42, 583–600. doi:10.1007/s00126-007-0125-7
- Morris, A.P., Ferrill, D. a., 2009. The importance of the effective intermediate principal stress (σ_2) to fault slip patterns. *J. Struct. Geol.* 31, 950–959. doi:10.1016/j.jsg.2008.03.013
- Morris, A., Ferrill, D.A., Henderson, D.B., 1996. Slip-tendency analysis and fault reactivation. *Geology* 24, 275–278.
- Munyai, M.R., Charlesworth, E.G., Dirks, P.H.G.M., 2011. Archaean gold mineralisation during post-orogenic extension in the New Consort Gold Mine, Barberton Greenstone Belt, South Africa. *South African J. Geol.* 114, 121–144.
- Mutemeri, N., 2001. Fluids and gold mineralization at Arcturus mine, Zimbabwe. *Zimbabwe Geol. Surv. Bull.* 100, 1–10.
- Nugus, M.J., Blenkinsop, T.G., Dominy, S.C., Robson, S., 2003. Enigmatic kinematics resolved in the Taurus Shear Zone Golden Pig Gold mine, Southern Cross, Western Australia - resource implications., in: *Proceedings of the 5th International Mining Geology Conference*. Bendigo, pp. 171–179.
- Oertel, G., 1965. The mechanism of faulting in clay experiments. *Tectonophysics* 2, 343–393. doi:10.1016/0040-1951(65)90032-6
- Oesterlen, P., Blenkinsop, T., 1994. Extension directions and strain near the failed triple junction of the Zambezi and Luangwa Rift zones, southern Africa. *J. African Earth Sci.* 18, 175–180.
- Oliver, N.H.S., Bons, P.D., 2001. Mechanisms of fluid flow and fluid-rock interaction in fossil metamorphic hydrothermal systems inferred from vein-wallrock patterns, geometry and microstructure. *Geofluids* 1, 137–162. doi:10.1046/j.1468-8123.2001.00013.x
- Oliver, N.H.S., Thomson, B., Freitas-silva, F.H., Holcombe, R.J., Rusk, B., Almeida, B.S., Faure, K., Davidson, G.R., Esper, E.L., Guimarães, P.J., Dardenne, M.A., 2015. Local and Regional

Mass Transfer During Thrusting , Veining , and Boudinage in the Genesis of the Giant Shale-
Hosted Paracatu Gold Deposit , Minas Gerais , Brazil. *Econ. Geol.* 110, 1803–1834.

Ord, A., Hunt, G.W., Hobbs, B.E., 2010. Patterns in our planet: defining new concepts for the
application of multi-scale non-equilibrium thermodynamics to Earth-system science. *Philos.*

Ord, A., Hobbs, B.E., Lester, D.R., 2012. The mechanics of hydrothermal systems: I. Ore systems
as chemical reactors. *Ore Geol. Rev.* 49, 1–44. doi:10.1016/j.oregeorev.2012.08.003

Ord, A., Munroe, M., Hobbs, B.E., 2016. Hydrothermal mineralising systems as chemical reactors.
Ore Geol. Rev. 79, 155–179.

Peng, Z., Gomberg, J., 2010. An integrated perspective of the continuum between earthquakes and
slow-slip phenomena. *Nat. Geosci.* 3, 599–607. doi:10.1038/ngeo940

Phillips, G.N., Groves, D.I., 1983. The nature of Archaean gold-bearing fluids as deduced from
gold deposits of Western Australia. *J. Geol. Soc. Aust.* 30, 25–39.
doi:10.1080/00167618308729234

Phillips, G.N., Powell, R., 2015. A practical classification of gold deposits, with a theoretical basis.
Ore Geol. Rev. 65, 568–573. doi:10.1016/j.oregeorev.2014.04.006

Pitcairn, I.K., Teagle, D.A.H., Craw, D., Olivo, G.R., Kerrich, R., Brewer, T.S., 2006. Sources of
metals and fluids in orogenic gold deposits: Insights from the Otago and Alpine schists, New
Zealand. *Econ. Geol.* 101, 1525–1546. doi:10.2113/gsecongeo.101.8.1525

Platt, J.P., Vissers, R.L.M., 1989. Extensional collapse of thickened continental lithosphere: A
working hypothesis for the Alboran Sea and Gibraltar Arc. *Geology* 17, 540–543.

Platten, I.M., Dominy, S.C., 1999. Re-evaluation of quartz vein history in the dolgellau gold-belt
North Wales, United Kingdom. *Geol. J.* 34, 369–391. doi:10.1002/(SICI)1099-
1034(199911/12)34:4<369::AID-GJ832>3.0.CO;2-G

Platten, I.M., Dominy, S.C., 2009. Geological mapping in the evaluation of structurally controlled
gold veins: a case study from the Dolgellau gold-belt, north Wales, UK, in: *Proc. Conf. World
Gold*. pp. 151–166.

Potma, W., Roberts, P.A., Schaubs, P.M., Sheldon, H.A., Zhang, Y., Hobbs, B.E., Ord, A., 2008.
Predictive targeting in Australian orogenic-gold systems at the deposit to district scale using
numerical modelling. *Aust. J. Earth Sci.* 55, 101–122. doi:Doi 10.1080/08120090701673328

Potts, G.J., Reddy, S.M., 2000. Application of younging tables to the construction of relative
deformation histories—1: Fracture systems. *J. Struct. Geol.* 22, 1473–1490.

- Poulsen, K.H., 1996. Lode gold, in: Eckstrand, O.R., Sinclair, W.D., Thorpe, R.I. (Eds.), *The Geology of North America*. Geological Society of America, pp. 323–328.
- Poulsen, H., Robert, F., 1989. Shear zones and gold: Practical examples from the southern Canadian Shield, in: Bursnall, J.T. (Ed.), *Mineralization and Shear Zones*, Geological Association of Canada, Short Course Notes 6. Montreal, pp. 239–266.
- Poulsen, K.H., Robert, F., Dube, B., 2000. Geological classification of Canadian gold deposits, *Bulletin of the Geological Survey of Canada*. doi:10.1126/science.ns-6.149S.521-a
- Raine, M.D., 2005. Polyphase deformation and the structural controls on economic gold occurrences within the Bendigo gold field, central Victoria, Australia. James Cook University.
- Ramsay, J.G., Graham, R.H., 1970. Strain variation in shear belts. *Can. J. Earth Sci.* 7, 786–813. doi:10.1139/e70-078
- Reches, Z., 1983. Faulting of rocks in three-dimensional strain fields II. Theoretical analysis. *Tectonophysics* 95, 133–156. doi:http://dx.doi.org/10.1016/0040-1951(83)90264-0
- Ridley, J., 1993. The relations between mean rock stress and fluid flow in the crust: With reference to vein- and lode-style gold deposits. *Ore Geol. Rev.* 8, 23–37. doi:10.1016/0169-1368(93)90026-U
- Riley, M.S., 2005. Fracture trace length and number distributions from fracture mapping. *J. Geophys. Res. B Solid Earth* 110, 1–16. doi:10.1029/2004JB003164
- Robert, F., Boullier, A.-M., Firdaous, K., 1995. Gold-quartz veins in metamorphic terranes and their bearing on the role of fluids in faulting. *J. Geophys. Res. Solid Earth* 100, 12861–12879. doi:10.1029/95JB00190
- Royden, L.H., 1993. The tectonic expression of slab pull at continental convergent boundaries. *Tectonics* 12, 303–325.
- Rutter, E.H., 1986. On the nomenclature of mode of failure transitions in rocks. *Tectonophysics* 122, 381–387. doi:10.1016/0040-1951(86)90153-8
- Sanderson, D.J., Marchini, W.R.D., 1984. Transpression. *J. Struct. Geol.* 6, 449–458. doi:http://dx.doi.org/10.1016/0191-8141(84)90058-0
- Sanderson, D.J., Nixon, C.W., 2015. The use of topology in fracture network characterization. *J. Struct. Geol.* 72, 55–66. doi:10.1016/j.jsg.2015.01.005
- Sanislav, I. V., Kolling, S.L., Brayshaw, M., Cook, Y.A., Dirks, P.H.G.M., Blenkinsop, T.G.,

Mturi, M.I., Ruhega, R., 2015. The geology of the giant Nyankanga gold deposit, Geita

Greenstone Belt, Tanzania. *Ore Geol. Rev.* 69, 1–16. doi:10.1016/j.oregeorev.2015.02.002

Sanislav, I. V., Brayshaw, M., Kolling, S.L., Dirks, P.H.G.M., Cook, Y.A., Blenkinsop, T.G., 2017.

The structural history and mineralization controls of the world-class Geita Hill gold deposit,

Geita Greenstone Belt, Tanzania. *Miner. Depos.* 52, 257–279. doi:10.1007/s00126-016-0660-1

Schaubs, P.M., Zhao, C., 2002. Numerical models of gold-deposit formation in the Bendigo–

Ballarat Zone, Victoria. *Aust. J. Earth Sci.* 49, 1077–1096. doi:10.1046/j.1440-

0952.2002.00964.x

Schaubs, P.M., Rawling, T.J., Dugdale, L.J., Wilson, C.J.L., 2006. Factors controlling the location

of gold mineralisation around basalt domes in the stawell corridor: insights from coupled 3D

deformation – fluid-flow numerical models. *Aust. J. Earth Sci.* 53, 841–862.

doi:10.1080/08120090600827496

Shan, Y., Fry, N., 2005. A hierarchical cluster approach for forward separation of heterogeneous

fault/slip data into subsets. *J. Struct. Geol.* 27, 929–936. doi:10.1016/j.jsg.2005.02.001

Sheldon, H.A., Micklethwaite, S., 2007. Damage and permeability around faults: Implications for

mineralization. *Geology* 35, 903. doi:10.1130/G23860A.1

Shepherd, T.J., Allen, P.M., 1985. Metallogenesis in the Harlech Dome, North Wales: A fluid

inclusion interpretation. *Miner. Depos.* 20, 159–168. doi:10.1007/BF00204560

Shepherd, T.J., Bottrell, S.H., Miller, M.F., 1991. Fluid inclusion volatiles as an exploration guide

to black shale-hosted gold deposits, Dolgellau gold belt, North Wales, UK. *J. Geochemical*

Explor. 42, 5–24. doi:10.1016/0375-6742(91)90058-3

Sibson, R., 1985. A note on fault reactivation. *J. Struct. Geol.* 7, 3–6.

Sibson, R., 1987. Earthquake rupturing as a mineralizing agent in hydrothermal systems. *Geology*

15, 710–704.

Sibson, R.H., Robert, F., Poulsen, K.H., 1988. High-angle reverse faults, fluid-pressure cycling, and

mesothermal gold-quartz deposits. *Geology* 16, 551–555. doi:10.1130/0091-

7613(1988)016<0551:HARFFP>2.3.CO;2

Smith, D.L., Evans, B., 1984. Diffusional crack healing in quartz. *J. Geophys. Res. Solid Earth* 89,

4125–4135. doi:10.1029/JB089iB06p04125

Stauffer, D., Aharony, A., 1994. *Introduction To Percolation Theory*. Taylor & Francis.

Stephens, J.R., Mair, J.L., Oliver, N.H., Hart, C.J., Baker, T., 2004. Structural and mechanical

controls on intrusion-related deposits of the Tombstone Gold Belt, Yukon, Canada, with comparisons to other vein-hosted ore-deposit types. *J. Struct. Geol.* 26, 1025–1041. doi:10.1016/j.jsg.2003.11.008

Stillwell, F.L., 1918. Replacement in the Bendigo quartz veins and its relation to gold deposition. *Econ. Geol.* 13, 100–111.

Sun, X., Zhang, Y., Xiong, D., Sun, W., Shi, G., Zhai, W., Wang, S., 2009. Crust and mantle contributions to gold-forming process at the Daping deposit, Ailaoshan gold belt, Yunnan, China. *Ore Geol. Rev.* 36, 235–249. doi:10.1016/j.oregeorev.2009.05.002

Sung, Y.-H., Ciobanu, C.L., Pring, a., Brügger, J., Skinner, W., Cook, N.J., Nugus, M., 2007. Tellurides from Sunrise Dam gold deposit, Yilgarn Craton, Western Australia: a new occurrence of nagyágite. *Mineral. Petrol.* 91, 249–270. doi:10.1007/s00710-007-0199-z

Tenthorey, E., Cox, S.F., Todd, H.F., 2003. Evolution of strength recovery and permeability during fluid–rock reaction in experimental fault zones. *Earth Planet. Sci. Lett.* 206, 161–172. doi:10.1016/S0012-821X(02)01082-8

Thakur, P., Srivastava, D.C., Gupta, P.K., 2017. The genetic algorithm : A robust method for stress inversion. *J. Struct. Geol.* 94, 227–239. doi:10.1016/j.jsg.2016.11.015

Thiele, S.T., Jessell, M.W., Lindsay, M., Ogarko, V., Wellmann, J.F., Pakyuz-Charrier, E., 2016a. The topology of geology 1: Topological analysis. *J. Struct. Geol.* 91, 27–38. doi:10.1016/j.jsg.2016.08.009

Thiele, S.T., Jessell, M.W., Lindsay, M., Wellmann, J.F., Pakyuz-Charrier, E., 2016b. The topology of geology 2: Topological uncertainty. *J. Struct. Geol.* 91, 74–87. doi:10.1016/j.jsg.2016.08.010

Tikoff, B., Fossen, H., 1993. Simultaneous pure and simple shear: the unifying deformation matrix. *Tectonophysics* 217, 267–283.

Tikoff, B., Greene, D., 1997. Stretching lineations in transpressional shear zones: an example from the Sierra Nevada Batholith, California. *J. Struct. Geol.* 19, 29–39.

Tikoff, B., Fossen, H., 1999. Three-dimensional reference deformations and strain facies. *J. Struct. Geol.* 21, 1497–1512. doi:10.1016/S0191-8141(99)00085-1

Tikoff, B., Blenkinsop, T., Kruckenberg, S.C., Morgan, S., Newman, J., Wojtal, S., 2013. A perspective on the emergence of modern structural geology: Celebrating the feedbacks between historical-based and process-based approaches. *Web Geol. Sci. Adv. Impacts Interact. Special Pa.* 65–119. doi:doi:10.1130/2013.2500(03)

- Townend, J., Zoback, M.D., 2000. How faulting keeps the crust strong. *Geology* 28, 399–402.
doi:10.1130/0091-7613(2000)28<399:HFKTCS>2.0.CO;2
- Tripp, G.I., Vearncombe, J.R., 2004. Fault/fracture density and mineralization: A contouring method for targeting in gold exploration. *J. Struct. Geol.* 26, 1087–1108.
doi:10.1016/j.jsg.2003.11.002
- Tunks, A.J., Selley, D., Rogers, J.R., Brabham, G., 2004. Vein mineralization at the Damang Gold Mine, Ghana: controls on mineralization. *J. Struct. Geol.* 26, 1257–1273.
doi:10.1016/j.jsg.2003.11.005
- Twiss, R.J., Moores, E.M., 2007. *Structural Geology*, 2nd Editio. ed. W.H. Freeman.
- Underhill, J.R., Woodcock, N.H., 1987. Faulting mechanisms in high-porosity sandstones; New Red Sandstone, Arran, Scotland. *Geol. Soc. London, Spec. Publ.* 29, 91–105.
doi:10.1144/GSL.SP.1987.029.01.09
- Van der Pluijm, B.A., Marshak, S., 2004. *Earth Structure: An Introduction to Structural Geology and Tectonics*. W.W. Norton.
- van Ryt, M.R., Sanislav, I. V., Dirks, P.H.G.M., Huizenga, J.M., Mturi, M.I., Kolling, S.L., 2017. Alteration paragenesis and the timing of mineralised quartz veins at the world-class Geita Hill gold deposit, Geita Greenstone Belt, Tanzania. *Ore Geol. Rev.* 0–1.
doi:10.1016/j.oregeorev.2017.08.023
- Vearncombe, J.R., 1998. Shear zones, fault networks, and Archean gold. *Geology* 26, 855.
doi:10.1130/0091-7613(1998)026<0855:SZFNAA>2.3.CO;2
- Vearncombe, J., Vearncombe, S., 1998. Structural data from drill core. *Aust. Inst. Geosci. Bull.* 22, 67–82.
- Vearncombe, J., Zelic, M., 2015. Structural paradigms for gold: do they help us find and mine? *Appl. Earth Sci.* 124. doi:10.1179/1743275815Y.0000000003
- Warren, J.D., Thébaud, N., Miller, J.M., Micklethwaite, S., 2015. Distinguishing between local versus regional extension as a control on orogenic gold mineralisation: The new 2.4Moz Castle Hill Camp, WA. *Precambrian Res.* 269, 242–260. doi:10.1016/j.precamres.2015.08.008
- Weinberg, R.F., van der Borgh, P., 2008. Extension and gold mineralization in the Archean Kalgoorlie Terrane, Yilgarn Craton. *Precambrian Res.* 161, 77–88.
- Weinberg, R.F., Hodkiewicz, P.F., Groves, D.I., 2004. What controls gold distribution in Archean terranes? *Geology* 32, 545. doi:10.1130/G20475.1

- Weiss, L. e., McIntyre, D.B., 1957. Structural geometry of Dalradian rocks at Loch Leven, Scottish Highlands. *J. Geol.* 65, 575–602.
- Witt, W., Vanderhor, F., 1998. Diversity within a unified model for Archaean gold mineralization in the Yilgarn Craton of Western Australia: An overview of the late-orogenic, structurally-controlled gold deposits. *Ore Geol. Rev.* 13, 29–64. doi:10.1016/S0169-1368(97)00013-9
- Woodcock, N.H., Underhill, J.R., 1987. Emplacement-related fault patterns around the Northern Granite, Arran, Scotland. *Geol. Soc. Am. Bull.* 98, 515–527. doi:10.1130/0016-7606(1987)98<515:EFPATN>2.0.CO;2
- Wyman, D.A., Cassidy, K.F., Hollings, P., 2016. Orogenic gold and the mineral systems approach : Resolving fact , fiction and fantasy. *Ore Geol. Rev.* 78, 322–335. doi:10.1016/j.oregeorev.2016.04.006
- Wyborn, L.A., Heinrich, C.A., Jaques, A.L., 1994. Australian Proterozoic mineral systems: essential ingredients and mappable criteria, in: *AusIMM Annual Conference, AusIMM Publ. Ser. 5 (94)*, Australian Institute of Mining and Metallurgy, Darwin, pp. 109–115.
- Yamaji, A., Sato, K., Tonai, S., 2010. Stochastic modeling for the stress inversion of vein orientations: Paleostress analysis of Pliocene epithermal veins in southwestern Kyushu, Japan. *J. Struct. Geol.* 32, 1137–1146. doi:10.1016/j.jsg.2010.07.001
- Yardley, B.W.D., 1986. Fluid Migration and Veining in the Connemara Schists, Ireland, in: Walther, J. V, Wood, B.J. (Eds.), *Fluid---Rock Interactions during Metamorphism*. Springer New York, New York, NY, pp. 109–131. doi:10.1007/978-1-4612-4896-5_5
- Yardley, B.W.D., Cleverley, J.S., 2013. The role of metamorphic fluids in the formation of ore deposits. *Geol. Soc. London, Spec. Publ.* 393, 117–134. doi:10.1144/sp393.5
- Žalohar, J., Vrabec, M., 2007. Paleostress analysis of heterogeneous fault-slip data: The Gauss method. *J. Struct. Geol.* 29, 1798–1810. doi:10.1016/j.jsg.2007.06.009
- Žalohar, J., Vrabec, M., 2008. Combined kinematic and paleostress analysis of fault-slip data: The Multiple-slip method. *J. Struct. Geol.* 30, 1603–1613. doi:10.1016/j.jsg.2008.09.004
- Žalohar, J., Vrabec, M., 2010. Kinematics and dynamics of fault reactivation: The Cosserat approach. *J. Struct. Geol.* 32, 15–27. doi:10.1016/j.jsg.2009.06.008

Figure Captions

Fig. 1. A spectrum of structures that may control hydrothermal mineralization. The top row (A to D) indicate planar features (mineralization as yellow polygons), the lower row (C to F) show linear features, emphasized by yellow ellipsoids lines.

Fig. 2. Planar deformation structures that may control gold mineralization: Top row shows individual features, middle row shows deformation zones, and lower row shows networks of zones, as labeled. The features are arranged within rows from discontinuous on the left to continuous on the right.

Fig. 3. Photographs of deformation zones related to gold mineralization, arranged in order from discontinuous to continuous deformation at the cm scale. The description of continuity, specified by scale, avoids ambiguities created by applying the terms “brittle” and “ductile” to these structures.

A) Quartz carbonate extensional vein with coarse gold, Sunrise Dam gold mine, formed during D4b (Table 1). This is an end-member example of discontinuous deformation at a cm scale.

B) Breccia from Sunrise Dam Gold Mine consisting of fuchsite-altered host rock fragments with quartz-carbonate infill, formed during to D4b (Table 1). The breccia is also an example of discontinuous deformation at a cm scale.

C) Quartz carbonate veins and S fabrics (dashed lines), indicating sinistral shear in the center of Star and Comet pit, Geita Gold Mine, Tanzania. Discontinuous and continuous deformation features coexist at the cm scale.

D) Sunrise Shear zone, open pit, Sunrise Dam Gold Mine, W. Australia. SC fabrics indicate reverse-sinistral shear during D3 (see Table 1). Discontinuous and continuous deformation features coexist at the cm scale.

E) Penetrative fabric forming zone of dominantly continuous shear at the cm scale, Tropicana gold deposit, Australia

F) Penetrative schistosity and continuous deformation at the m scale, Cornishman open pit, Southern Cross greenstone belt, W. Australia

Fig. 4. Network Topology. Branches connect I, Y and X nodes. NY, NX are numbers of Y and X

nodes respectively. ? indicate an ambiguity in how the three labeled branches can be joined into traces. Which of the upper query larks join to the lower query mark? There is no objective criterion to allow unique traces to be determined. This example is based on an underground exposure of mineralized quartz-carbonate veins in the Astro lode at Sunrise Dam gold mine, W. Australia, which were coeval with mineralization as demonstrated by common alteration and infill assemblages, and by mutually cross-cutting relationships.

Fig. 5. Relationships between syn-mineralization ore bodies (OB), lineations (L) and vorticity vectors (V) in pure shear and simple shear dominated deformation zones. Grey cube indicates undeformed state, black shows deformed state. A) In pure shear dominated zones, V is parallel to L and orebodies also form in this direction. B, C) In Simple-shear dominated zones, L is perpendicular to V. B) Where permeability is created by the L fabric, ore bodies will form in this direction C) where geometrical irregularities and intersecting fabrics (purple planes) occur, ore bodies may form parallel to V.

Fig. 6. Cartoon to show kinematic controls on ore body geometry at Golden Pig mine, Southern Cross greenstone belt, Yilgarn craton, Australia. Lineation and vorticity vector plunge very gently to the South, indicating a pure-shear dominated shear zone. Permeability and/or extension lead to the elongation of ore bodies in this direction. The geometrical controls are similar to Case A in Fig. 5.

Fig. 7. Equal area, lower hemisphere stereoplots of structural elements at Renco, Shamva and Arcturus mines, Zimbabwe craton, showing the variable relationships between ore bodies (black triangles) lineations (black circles) and vorticity vectors (red circles). Great circles are shear planes. All structures have been determined from eigenvector analysis of individual measurements. At Renco and Shamva, lineations are perpendicular to the vorticity vector: simple shear is dominant. At Renco, ore bodies form parallel to lineation because of kinematic and/or fabric controls. Arrow shows reverse movement. At Shamva, ore bodies form perpendicular to lineation and parallel to the vorticity vector, which is also the direction of maximum permeability due to intersections of shears. At Arcturus, lineations are parallel to the vorticity vector (pure shear dominant): ore bodies also form in this direction. Sinistral strike-slip shear characterizes both Shamva and Arcturus.

Fig. 8. Shear zone and fault networks that form in multiple orientations simultaneously. Cubes indicate undeformed state; principal strain axes are parallel to the edges of the white deformed cuboids. A, B: shear zone networks formed in constriction and flattening respectively. C, D: fault

zone networks formed in constriction and flattening respectively. Figure based on Choukroune and Gapais (1983); Krantz (1988); Healy et al. (2015).

Fig. 9. Two dimensional Mohr diagrams showing failure conditions for intact rock and failed surfaces in reactivation. a) The failure envelop for the failed surface has the same coefficient of internal friction as intact rock, but no cohesion. The optimum surface for reactivation is represented by an asterisk. Planes represented by any point on the blue sector of the Mohr circle can be reactivated. Colours show slip tendency from red (high) to green (low) b) The relationship between planes that can be reactivated and the maximum principal stress for the stress state shown in (a). Any plane between the two shown can be reactivated. c) The failure envelop for the failed surface has the same cohesion but a lower coefficient of internal friction. As in (a), surfaces in a range of possible orientations can be reactivated. d) Reactivation of some planes as only possible for negative least principal effective stresses: the Mohr circle shown is one example.

Fig. 10. Lower hemisphere equal area stereoplots of slip (upper row) and dilation tendencies (lower row) shown at poles to planes. White numerals show orientations of principal stresses. Diagrams shown for $\Phi = (\sigma_2 - \sigma_3)/(\sigma_1 - \sigma_3) = 0, 0.5$ and 1. The red areas of high slip and dilation tendency show that a variety of orientations can be reactivated for any stress state, and that the pattern changes as a function of Φ .

Fig. 11. The open system reactor concept for hydrothermal mineralization, from Ord et al., (2012). Feedback loops make this system non-linear, and give rise to multifractal properties of mineral distributions, for example.

Fig. 12. Asian Stress States from the World stress map (Heidbach et al., 2008). Stress states are separated into normal (red), strike-slip (green) and thrust fault (blue). Lines show the azimuth of maximum horizontal stress. Stress determination methods are shown in the key. In accretionary orogens (e.g. Sumatra-Indonesian and Philippine arcs), collisional orogens (e.g. the Himalayas) and intraplate orogens (e.g. the Tian Shan mountains) there are combinations of normal, strike slip and thrust fault stress states at all depths in the crust.

Fig. 13. Workflow for structural analysis of gold deposits

Table 1.

Deformation and intrusive events at Sunrise Dam Gold Mine

1
2
3
4
5
6
7
8
9
10
11
12
13
14
15
16
17
18
19
20
21
22
23
24
25
26
27
28
29
30
31
32
33
34
35
36
37
38
39
40
41
42
43
44
45
46
47
48
49
50
51
52
53
54
55
56
57
58
59
60
61
62
63
64
65

Figure 1

T
A
B
U
L
A
R

E
L
O
N
G
A
T
E

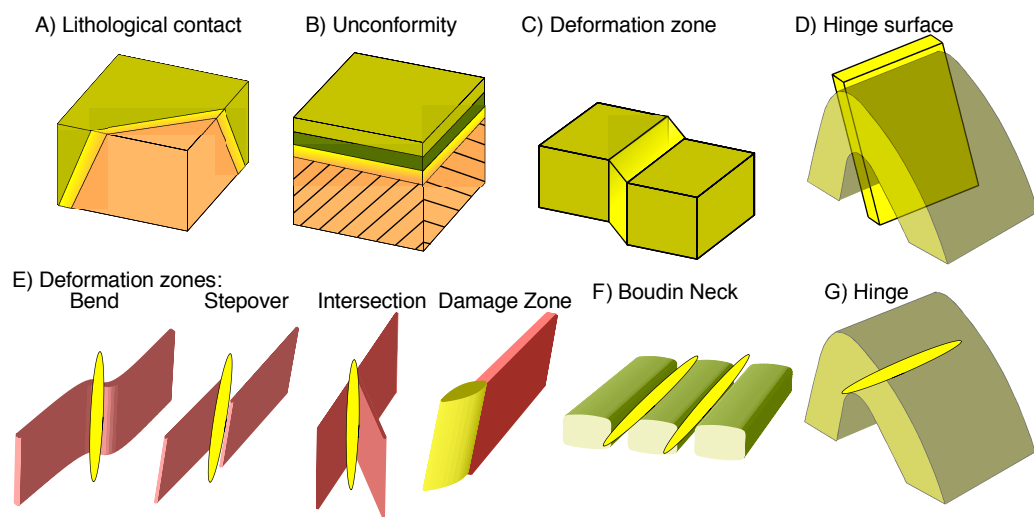


Figure 2

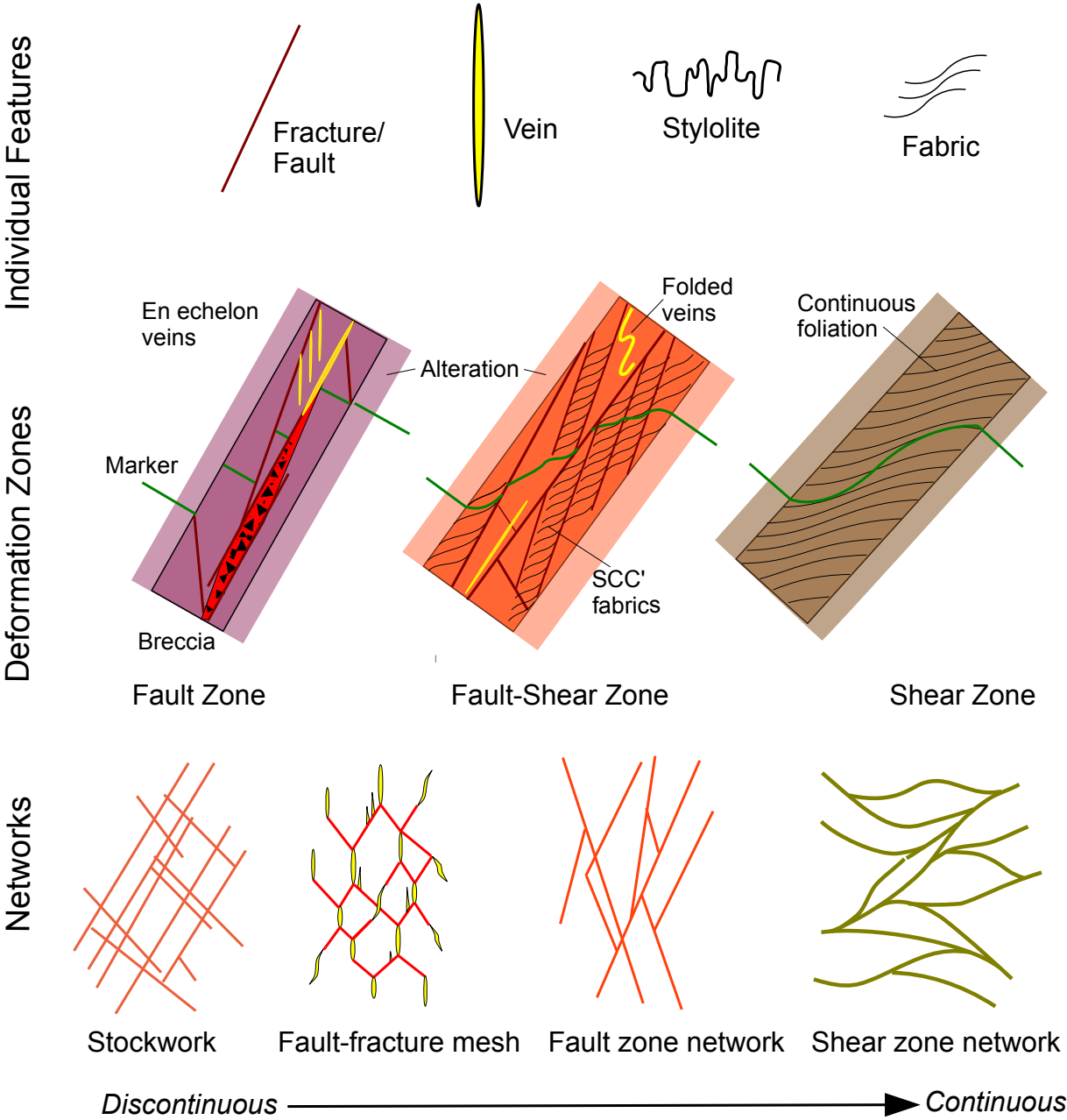


Figure 3



Discontinuous

Continuous

Figure 4

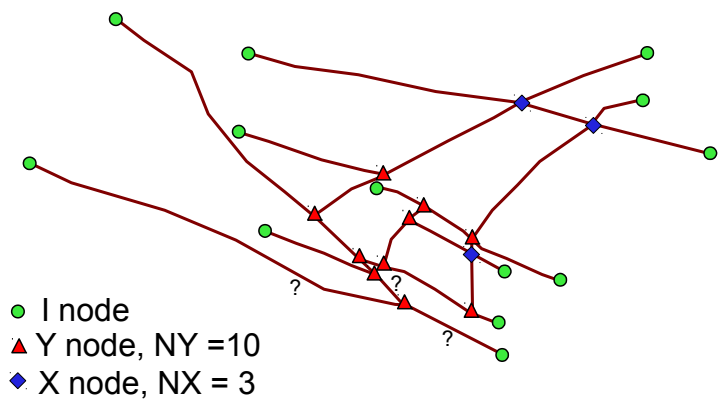


Figure 5

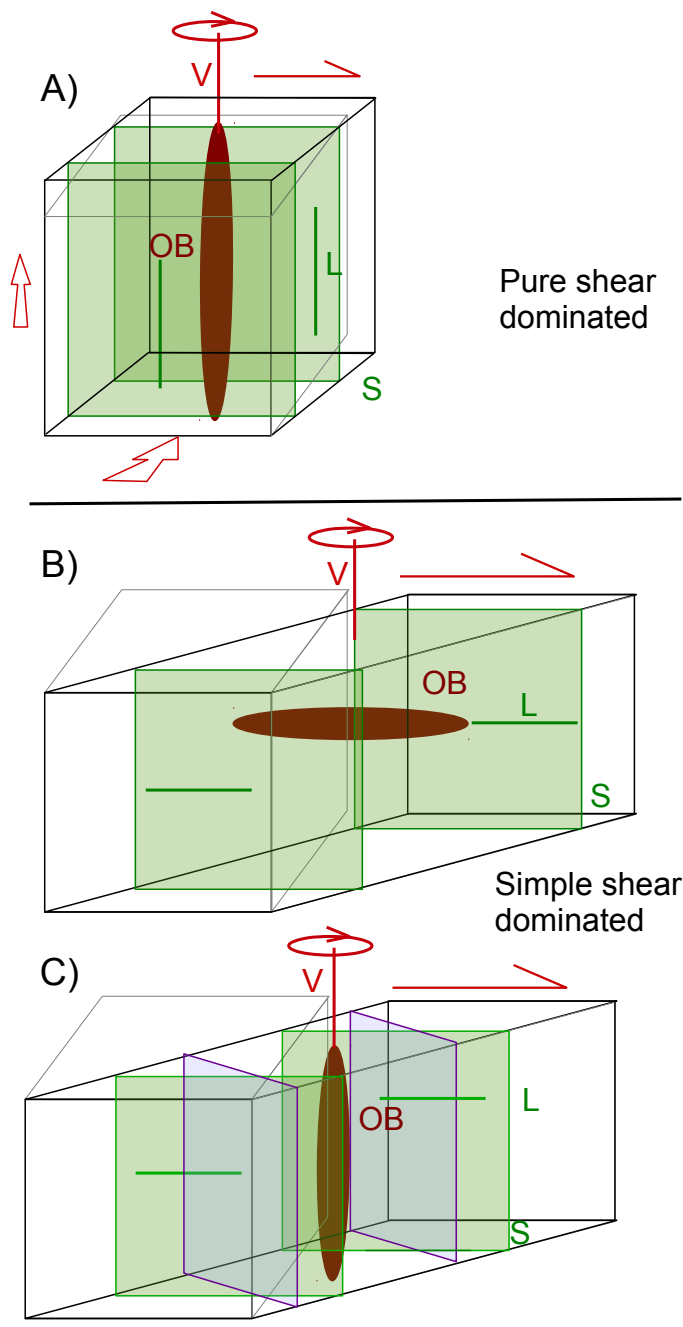


Figure 6

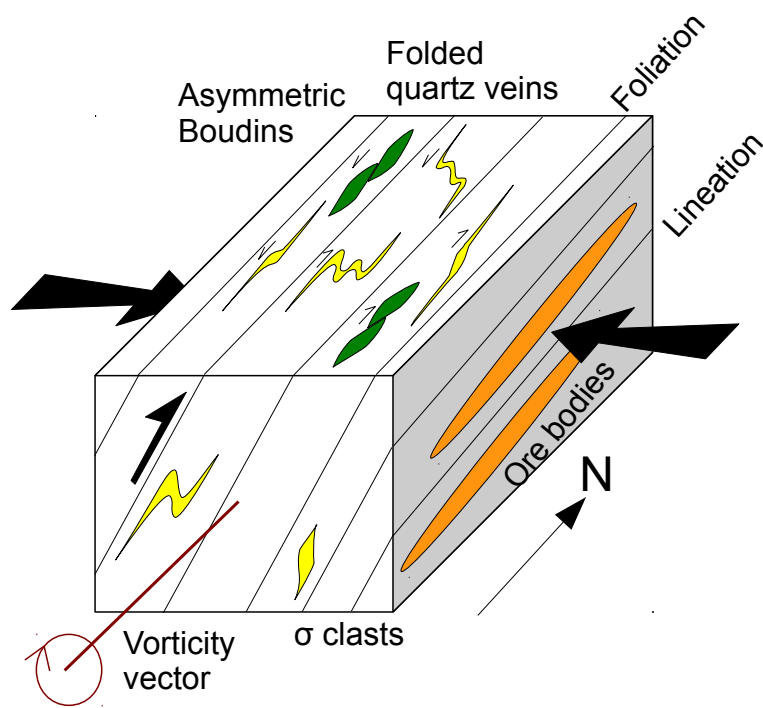


Figure 7

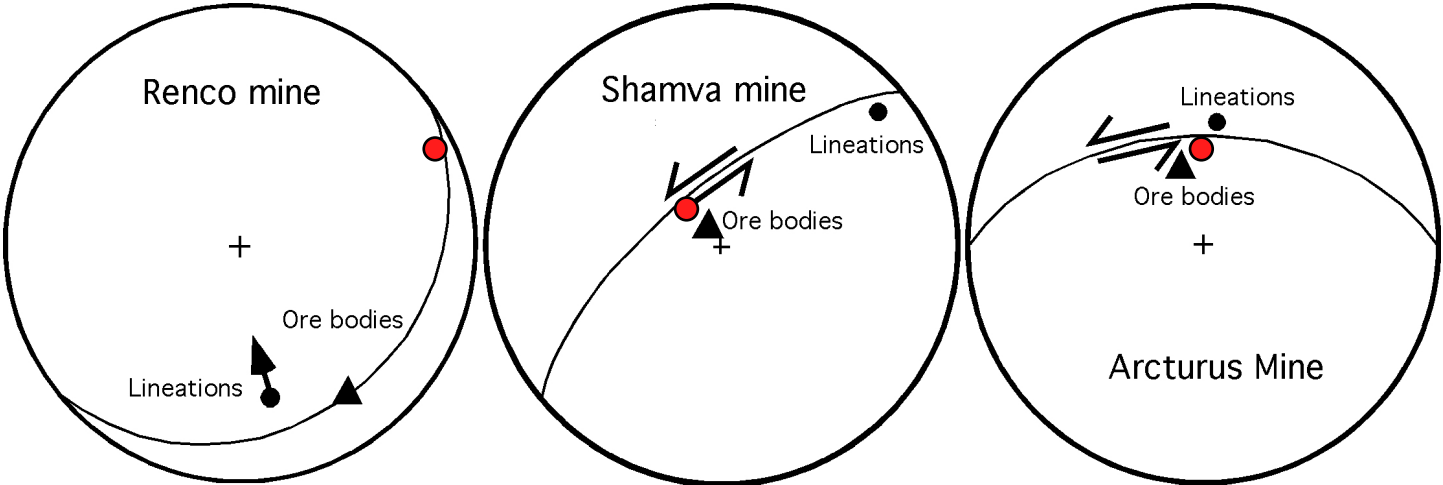
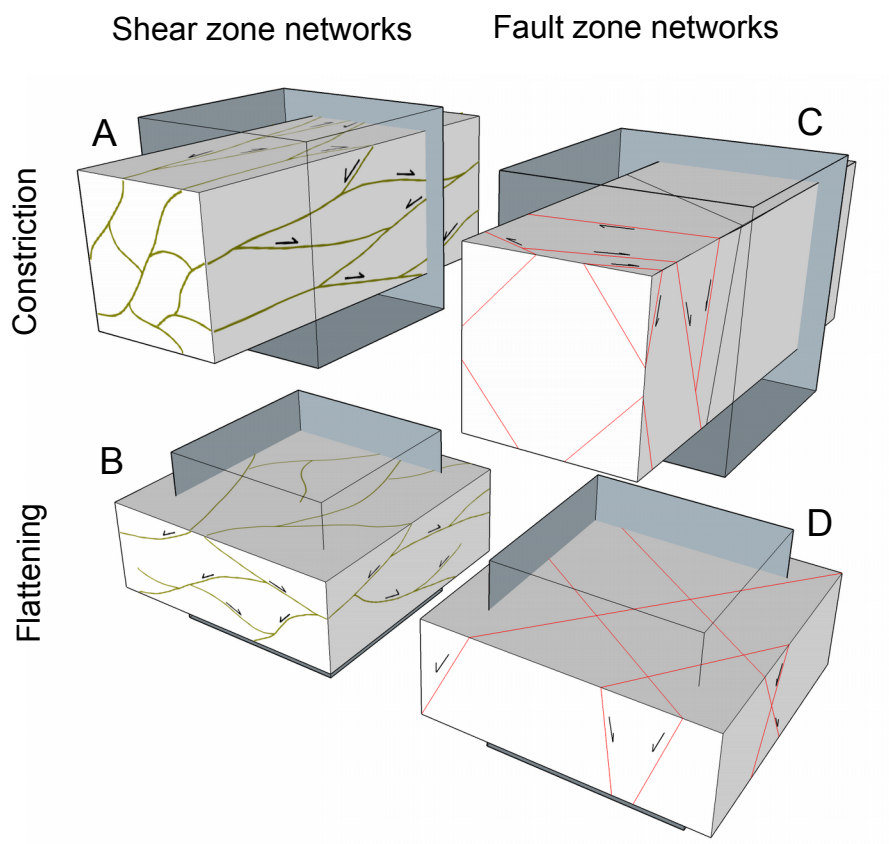


Figure 8



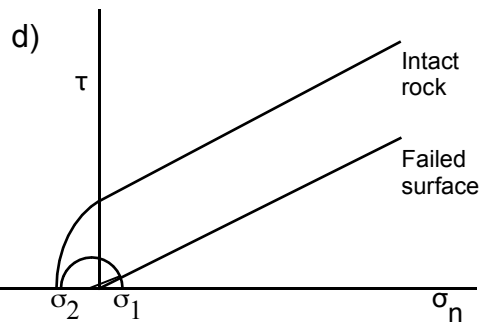
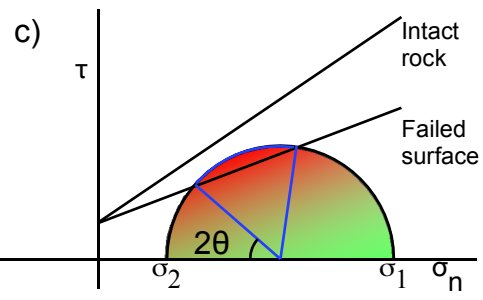
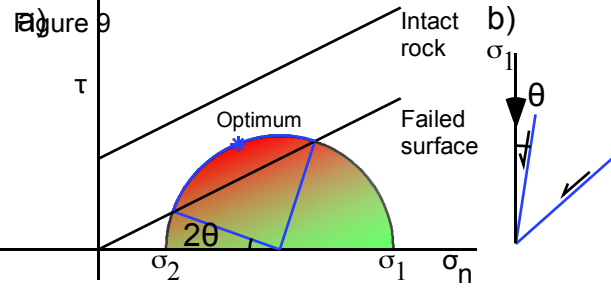


Figure 10
Dilation
Tendency

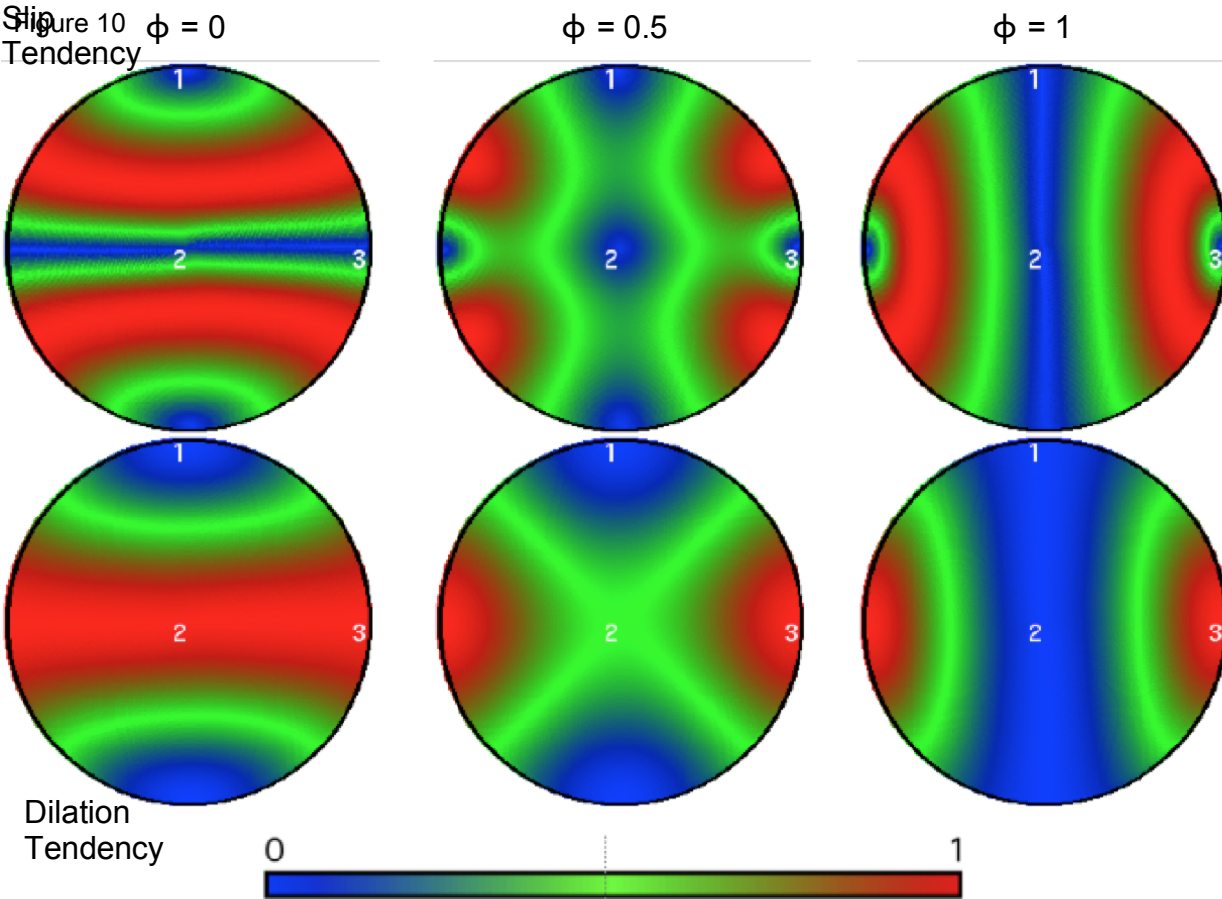


Figure 11

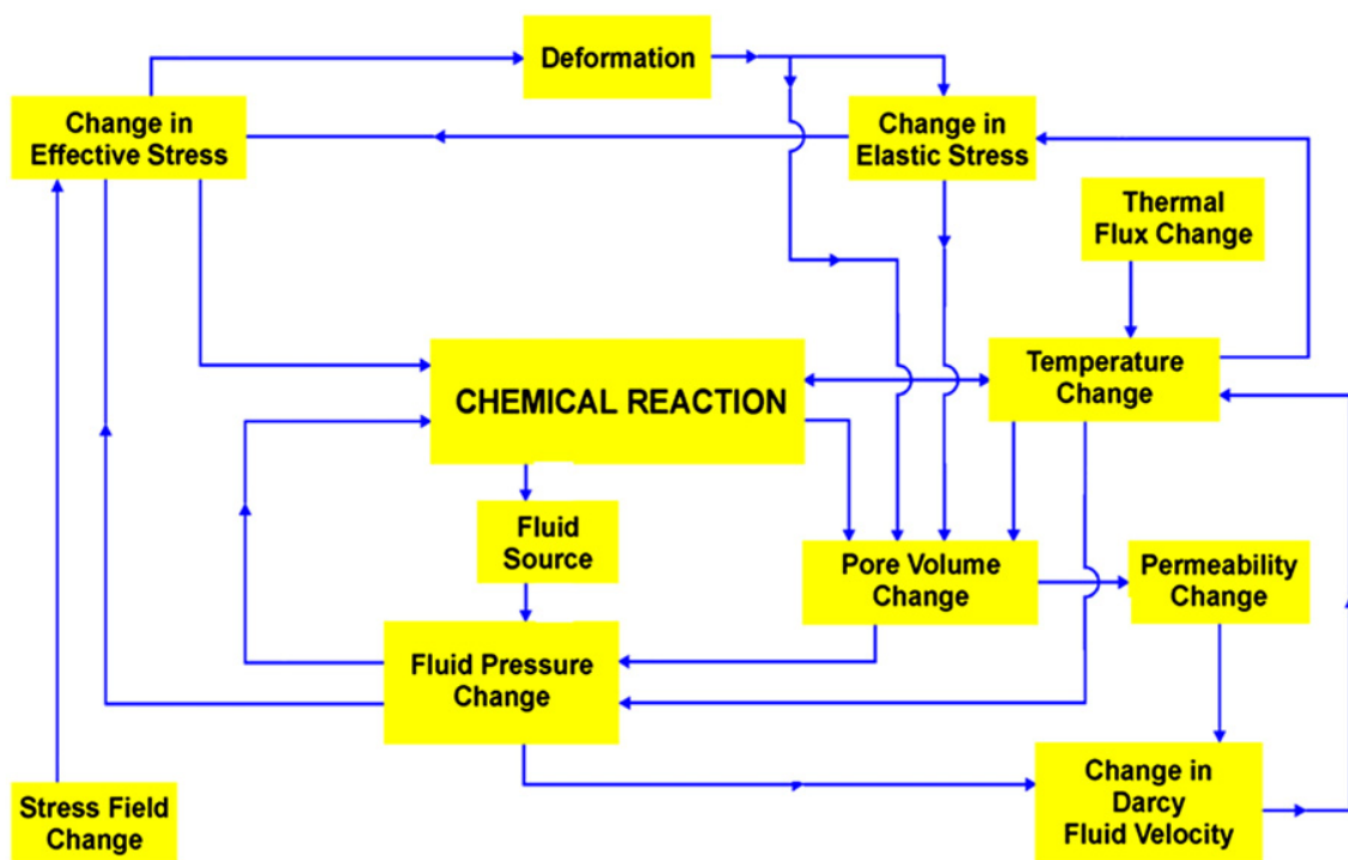


Figure 12

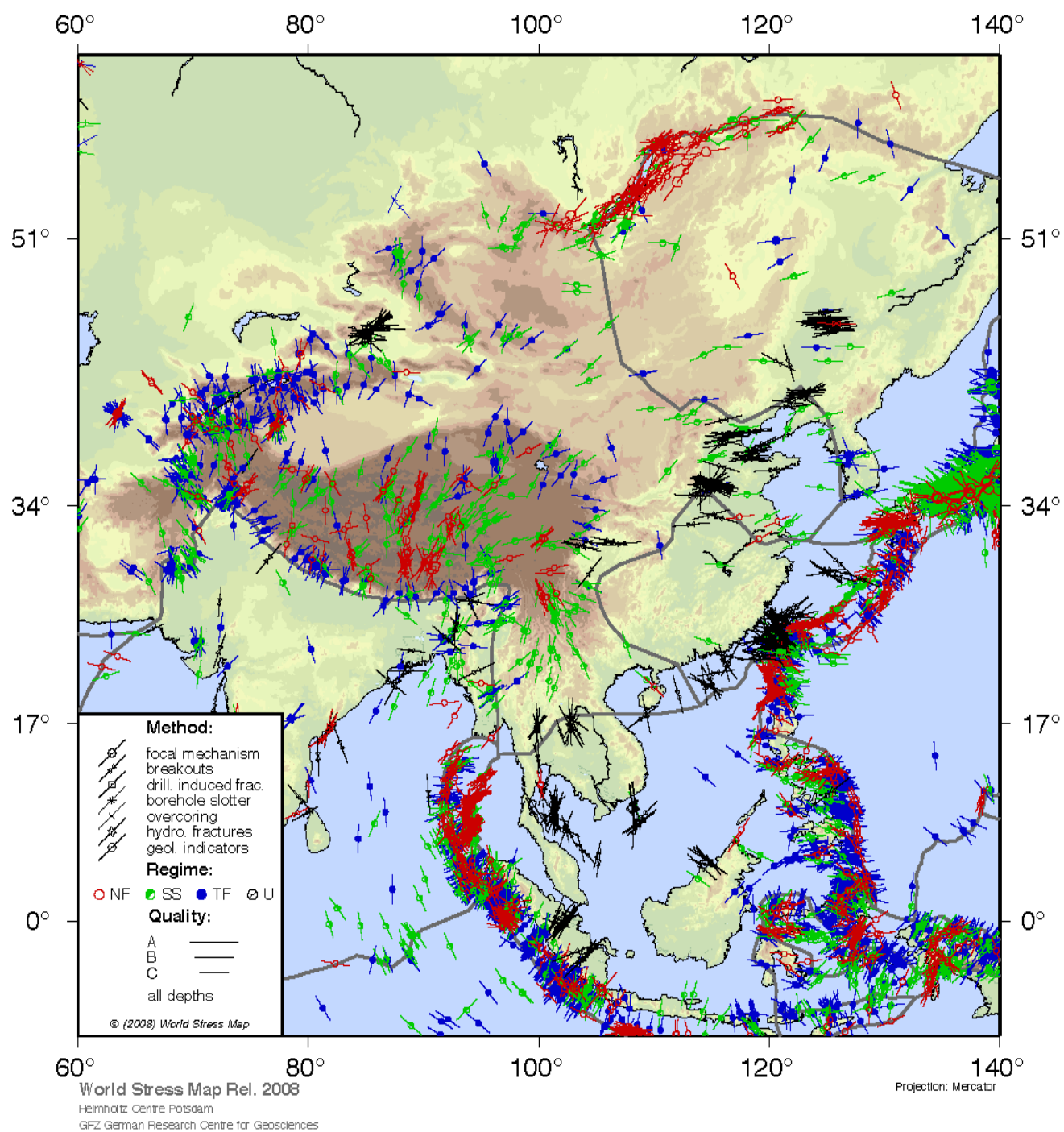


Figure 13

Data acquisition: Structural database, GIS, 3D software

Surface Mapping
Underground Mapping
Core logging
Microstructures
Geophysics
Geochemistry

Geometrical Analysis

Deformation zone geometry

Network geometry and Topology

3D Ore body geometry: *UVW* axes

Kinematic Analysis

Displacement history

Kinematic (strain) axes and realtive timing; history

Dynamic Analysis

Paleostress History, including fluids

Mechanical Analysis

Rheology

Numerical Modelling

Synthesis

Structural controls on ore bodies

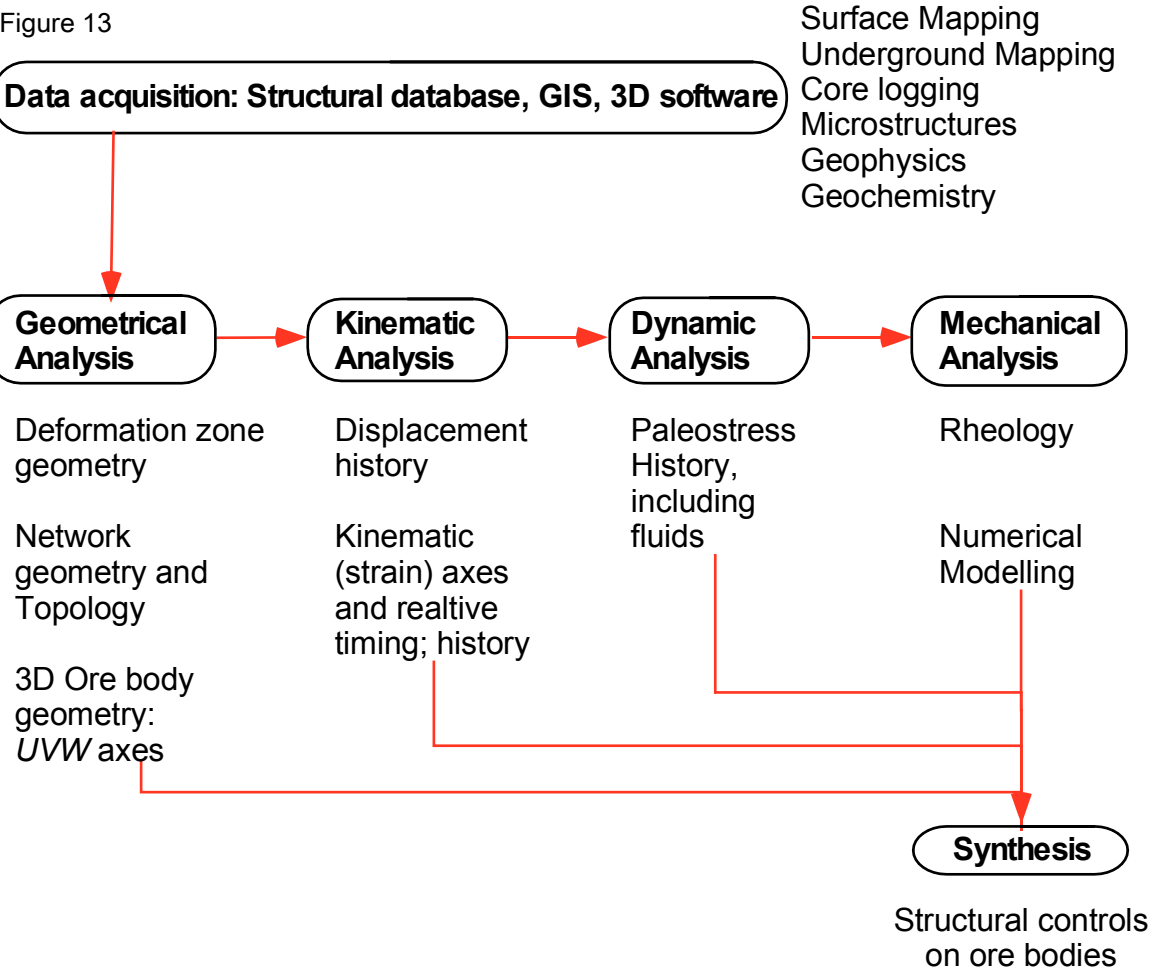


Table 1. Deformation and Intrusive events at Sunrise Dam Gold Mine, WA.

Event	Kinematics	Regime	σ_1	ϕ
Extension	E-W extension			
D6?	Dextral conjugate faulting			
D5	Sinistral faulting	Strike-slip	SE	0.95
D4b	Dextral faulting (late stage) Reactivation and extension			
D4a	Dextral faulting (early stage)	Strike-slip	ENE	0.95
Porphyry	Dyke Intrusion 2674 ± 3 Ma			
D3	Thrusting and sinistral wrenching	Strike-slip	SE	0.5
Porphyry				
D2	Regional EW shortening			
D1	NW thrusting or extension			